ACS APPLIED MATERIALS & INTERFACES

www.acsami.org

Review

Metal–Organic Frameworks in Agriculture

Sara Rojas,* Antonio Rodríguez-Diéguez, and Patricia Horcajada*

Cite This: *ACS Appl. Mater. Interfaces* 2022, 14, 16983–17007

Read Online

ACCESS | Metrics & More | Article Recommendations

ABSTRACT: Agrochemicals, which are crucial to meet the world food qualitative and quantitative demand, are compounds used to kill pests (insects, fungi, rodents, or unwanted plants). Regrettably, there are some important issues associated with their widespread and extensive use (e.g., contamination, bioaccumulation, and development of pest resistance); thus, a reduced and more controlled use of agrochemicals and thorough detection in food, water, soil, and fields are necessary. In this regard, the development of new functional materials for the efficient application, detection, and removal of agrochemicals is a priority. Metal–organic frameworks (MOFs) with exceptional sorptive, recognition capabilities, and catalytical properties have very recently shown their potential in agriculture. This Review emphasizes the recent advances in the use of MOFs in agriculture through three main views: environmental remediation, controlled agrochemical release, and detection of agrochemicals.

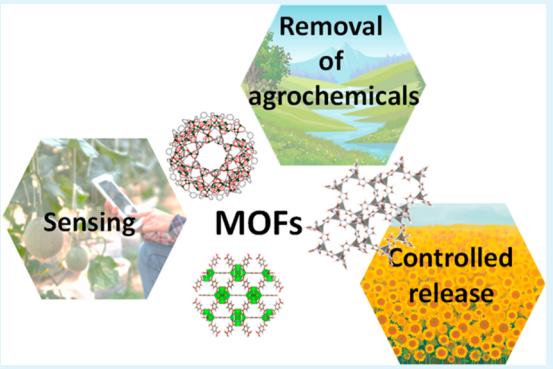

KEYWORDS: *metal–organic frameworks, agrochemicals, controlled release, selective adsorption and degradation, sensing*

1. CURRENT CHALLENGES OF AGRICULTURE

Agrochemicals or agrichemicals (primarily fertilizers and pesticides) have become a fundamental part of today's agricultural systems in order to fulfill the huge requirement of food. Agrochemicals can be classified on the basis of various principles, such as toxicity, target, chemical composition and formula, mode of entry or action, and source. Here, we will classify them according to their mode of action, although their toxicity, target, and origin will also be discussed. Thus, agrochemicals can be divided into pesticides (insecticides, herbicides, fungicides, rodenticides, algaecides, molluscicides, and nematicides), fertilizers (mainly supplying macronutrients: N, P, and K), soil conditioners (improving the soil's physical and mechanical qualities), liming (Ca and Mg) and acidifying agents, and plant growth regulators (also known as phytohormones).

With a dramatic increase after the second World War,[1] the intensive use of agrochemicals has deteriorated the quality of ecosystems (living beings, groundwaters, soils) by impacting human health and, in recent years, leading to the development of pesticide-resistant strains.[2−4] Over the period of 2011−2018, pesticide sales were around 360,000 tons per year only in the European Union (EU) with the major groups sold being fungicides, herbicides, and bactericides. This is particularly crucial since, according to the Food and Agriculture Organization (FAO) of the United Nations, agriculture occupies about 38% of Earth's terrestrial surface.[5] High and repeated doses of hazardous agrochemicals are routinely used to protect crops against pests (insects, fungi, unwanted plants, and others) and boost food productivity (e.g., increasing the number of times per year a crop can be grown on the same territory). With a global population projected to rise above 9.7 billion by 2050, food security is of increasing importance. Herbicides are the most widely used pesticides, comprising >40% of total use, while insecticides and fungicides constitute approximately 30% and 20%, respectively. Pesticide/fertilizer pollution patterns are well-established with a major pollution peak taking place a few days or weeks after agrochemical application.[6] Ideally, their toxic effect should be limited to both the target area and organisms. However, the lack of specificity of agrochemicals and their widespread use (i.e., in 2018 almost 400,000 tons of pesticides were sold in Europe)[7] allow them to leach out of the soil and enter surface water and groundwater; therefore, they are even present in drinking water.[8]

On the basis of their application methods, between 10% and 75% of the pesticides do not reach their targets,[9,10] resulting in frequent contamination of terrestrial and aquatic environments.[9−11] The EU Drinking Water Directive sets the general drinking water quality standard for added concentrations of pesticides and their metabolites to be less than 0.5 $\mu g \cdot L^{-1}$. Remarkably, most of the studies in this field report that ∼80%

Received: January 11, 2022
Accepted: March 15, 2022
Published: April 8, 2022

of the studied pesticides are found in concentrations much higher than the EU water quality standard (e.g., 3-fold higher concentrations of tebufenpyrad and pendimethalin in the Louros River in Greece,[12] 21- and 26-fold higher concentrations of glyphosate and aminomethylphosphonic acid (AMPA) in the area of Zurich, Switzerland,[13] 40-, 25-, and 20-fold higher concentrations of amitrole, diuron, and terbuthylazine in the Arc River in France, respectively,[14] and 8-, 12-, 16-, and 25-fold higher concentrations of oxadiazon, pretilachlor, bentazone, and 2-methyl-4-chlorophenoxyacetic acid (MCPA) in the Rhône River in France, respectively,[15] among others).

Despite the strict EU regulation, pesticides continue enter the food chain through water and food. Regarding other regions, the problem is magnified. For example, it is predicted that in 2050 the major part of global chemical sales will take place in Asia. During the last two decades, South-East Asian countries have shown a strong industrial growth in agriculture.[16] However, the vast majority of these countries lack the capacity to handle chemical management issues and, furthermore, they still need to develop legislation, institutions, and general awareness. Therefore, this should be considered a global environmental problem. In terms of acute toxicity to humans, many agrochemicals manifest their toxicity through biochemical and functional actions in the central and peripheral nervous system. Also, although not always easy to identify, there is evidence that links long-term exposure to some pesticides with chronic illnesses, including dermal, respiratory, liver, and kidney disorders,[17] fertility difficulties,[18,19] postponed neuropathy,[20] and cancer (e.g., sarcoma, lung, brain, gonads, liver, digestive system, and urinary tract).[20,21] In this sense, it is likely that the scale and outcome of pesticide-associated chronic effects are underestimated as the symptoms of such poisonings may be incorrectly attributed to other affects. Aside from toxicity to humans, in terms of environmental costs, the unsystematic use of agrochemicals increases pest and disease resistance, diminishes nitrogen fixation and soil biodiversity, and increases the bioaccumulation of pesticides.[22] Finally, the loss of livestock to resistant bacterial diseases also represents a considerable waste of water and energy investment as well as capital.

Apart from pesticides, fertilizers are among the major contributors to raise crop yield, and therefore, their use has been exponentially enhanced over the past decades (annually >3 million tons have been imported into the EU since 2015).[23] However, as for pesticides, the use of chemical fertilizers is limited by their poor specificity, increasing both the environmental and production costs (between 50% and 70% of total applied nitrogen is lost by volatilization[24,25] and 5−10% is lost by leaching).[26] Further, inefficiencies in the production of food are further intensified by food waste (i.e., ∼33−50% of global manufactured food spoils as consequence of microbial contamination).[27] The actual scenario of the inefficient use of fertilizers and intensive irrigation, biocides, and processed food is stressing ecosystems and leading to significant environmental collateral injuries (e.g., increasing soil erosion and degradation, loss of biodiversity, rising water withdrawals, reducing water quality, eutrophication, disruption of global nutrient cycles, and increasing the energy consumption and greenhouse gas emissions).[5] All the above suggests that water, food, nature, and animal and human health are inextricably linked to the agri-food systems.

2. NANOTECHNOLOGY AS A NOVEL APPROACH IN AGROCHEMICAL DEVELOPMENT

The increase of society's concern regarding the potential damage of agrochemical application in agricultural production has challenged industry and researchers to search for new efficient and safer methods against insect pests, infections, and unwanted plants or weeds. In this sense, nanotechnology research has recently received an increasing attention in agriculture. With the general aim of developing delivery nanosystems for agrochemicals,[28,29] nanopesticides and nanofertilizers have been proposed as a novel class of plant protection and growth products that promise a number of benefits to agriculture, the environment and, finally, human health. One of their key drivers is the important reduction in the quantity of agrochemicals necessary to guarantee crop protection and growth, which may be achieved by different ways, such as (i) improved apparent solubility and stability of photo- and thermolabile agrochemicals or active ingredients (AIs), (ii) controlled release and targeted delivery of AIs, and (iii) enhanced bioavailability and adhesion (Figure 1).

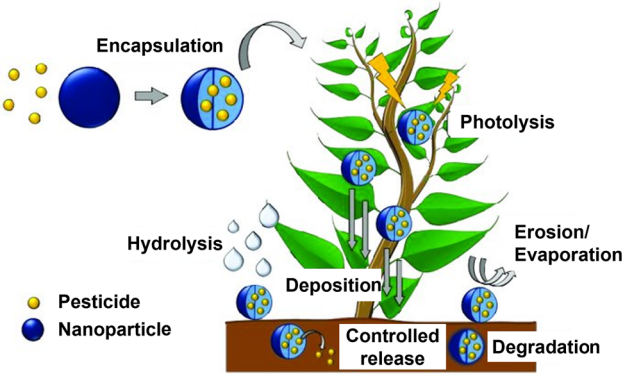

Figure 1. Application of nanotechnology in agriculture. Adapted from ref 39. Copyright 2017 MDPI.

Nanocarriers of agrochemicals of different natures have been described, including the known "soft" nanoparticles (NPs) (e.g., polymers, lipid, and nanoemulsions) as well as "hard" nanomaterials, such as silica NPs,[30−34] nanoclays,[35] TiO_2,[36] carbon nanotubes,[37] or graphene oxides.[38] Nanocarriers are mainly applied in plant nutrition with the final objective of an increased efficiency of the actually used fertilizers either by enhancing the administration of elements that are poorly bioavailable (P, Zn) or by reducing losses of mobile nutrients to other natural environments (nitrate). However, long-term instability, subsequent burst agrochemical release, and associated toxicity are some of the major drawbacks that need to be addressed.

3. METAL−ORGANIC FRAMEWORKS AS PROMISING MATERIALS IN AGRICULTURE

Among the novel technologies proposed in agriculture, metal−organic frameworks (MOFs) have gained a significant role in the fields of the elimination of agrochemicals (adsorption and/or photodegradation) and sensing. MOFs are considered to be a remarkable class of highly porous coordination polymers, containing inorganic nodes (e.g., atoms, clusters, or chains) and organic linkers (e.g., carboxylates, nitrogenated, or phosphonates), that assemble into multidimensional periodic lattices.[40] MOFs have been proposed for many societal and

https://doi.org/10.1021/acsami.2c00615
ACS Appl. Mater. Interfaces 2022, 14, 16983−17007

industrially relevant applications, such as adsorption,[41] separation,[42] magnetism,[43] luminescence,[44] conductivity,[45] sensing,[43] catalysis,[46] energy,[47] drug delivery,[48] etc. In particular, MOFs are promising materials in agriculture due to their interesting properties: (i) versatile hybrid compositions, which allow a huge variety of combinations, (ii) large specific surface areas and pore volumes, related to exceptional sorption capacities, (iii) simply functionalizable cavities, where specific host−guest interactions may occur, (iv) synthesis at large scale (some of them are already commercialized), and (v) an adequate stability profile, so they are stable enough to accomplish their function and, after being degraded, prevent associated toxicity in animals/plants due to their accumulation.

Different strategies have been reported in the use of MOF-type materials in agriculture. In particular, related to agrochemicals, MOFs have been proposed (i) in water remediation through the elimination (adsorption/degradation) of agrochemicals or derived products, (ii) as carriers for the controlled release of agrochemicals, and (iii) as sensors for the determination of these molecules in water or food (Figure 2). While not many reviews have detailed the use of MOFs in the elimination of agrochemicals as contaminants in water[49−53] or their potential in the detection and quantification of these potentially toxic molecules,[51,54,55] the use of MOFs as agrochemical delivery systems is a very recent research field, initiated in 2015.[56] Grouped by their function, this Review will discuss the MOFs and MOF-based composites that have been investigated to date in the agricultural domain. In order to give a broad spectrum of benefits and drawbacks of the use of each material, particular features of each structure and its properties are also included. In the text, the most original, interesting, and promising MOFs in agriculture will be highlighted, although all the reports currently found in the literature are summarized in Tables 1 to 3.

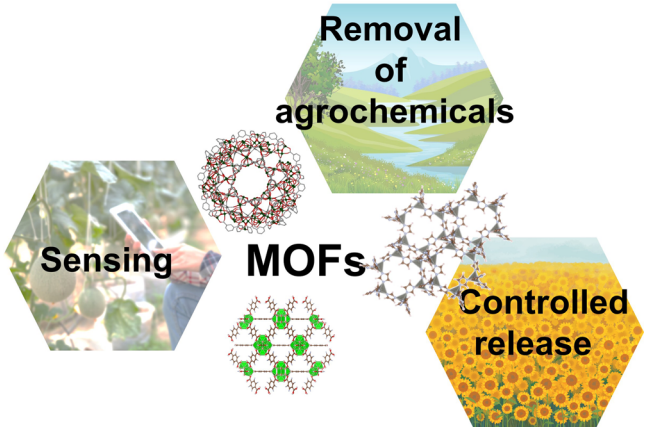

Figure 2. Proposed application related to agrochemicals and MOFs: environmental remediation, controlled release, and detection/quantification of agrochemicals.

4. MOFs IN ENVIRONMENTAL REMEDIATION: AGROCHEMICALS ELIMINATION

In recent years, MOFs have exponentially been investigated for the removal (mainly adsorption or degradation processes) of different contaminants from water. Originally, this field was focused on the removal of organic dyes, although recently, agrochemicals have also been included as target contaminants due to their increasing presence in natural waters and their severe toxicity to living beings. Thus, an increase in the number of reports dealing with the elimination of different agrochemicals using MOFs has been reported (Figure 3), including (i) **herbicides**: alachlor, atrazine (ATZ), bentazon, chipton, clopyralid, 2,4-dichlorophenoxyacetic acid (2,4-D), diuron (DUR), glufosinate (GLU), glyphosate (GLY), gramoxone, isoproturon (IPU), mecoprop, paraquat, quizalofop-P-ethyl (QPE), and tebuthiuron; (ii) **fungicides**: propiconazole and thifluzamide (THI); (iii) **insecticides**: chlorantraniliprole, chlorpyrifos, cyhalothrin, diazinon, dichlorvos, dimethoate, ethion, fenamiphos, fenitrothion, malathion methyl, metrifonate, nitenpyram (NIT), paraoxon, parathion methyl, prothiofos, thiamethoxam, several neonicotinoids (NND, acetamiprid, clothianidin, dinotefuran, imidacloprid, NIT, thiacloprid, and thiamethoxam), and organophosphorus pesticides (OP, diazinon, ethoprop, isazofos, methidathion, phosalone, profenofos, sulfotep, and triazophos). Table 1 summarizes the reported studies regarding agrochemical removal using MOFs and MOF-based composites with a summary of the conditions and results of each study (on the basis of the reported data presented by the authors).

4.1. Adsorption Processes. Regarding the adsorption of herbicides, the first study was published by Jung et al. in 2013 for the removal of 2,4-D using the MIL-53(Cr) material ([Cr(OH)(BDC)]; H_2BDC: benzene-1,4-dicarboxylic acid, pore size of ∼8 Å).[57] MIL-53(Cr) exhibited an efficient and fast adsorption (556 $mg·g^{-1}$ in 1 h) with an adsorption capacity much higher than that of activated carbon (286 $mg·g^{-1}$) or zeolite (256 $mg·g^{-1}$). Importantly, the adsorption of 2,4-D at a very low concentration is 5-fold greater that of activated carbon at a plateau concentration, demonstrating the utility of MIL-53(Cr) in commercial uses for consumed water with low 2,4-D levels. Finally, the recyclability of MIL-53(Cr), after washing the MOF with a mixture of water/ethanol, was also noticeable after 3 cycles, suggesting the potential application of this MOF on the herbicide's removal. In a more recent work, a series of furan-thiophene derived from Cr-MOF MIL-101(Cr) ($[Cr_3(O)X\text{-}(BDC)_3(H_2O)_2]$, X = OH or F; Brunauer−Emmett−Teller surface area (S_{BET}) ∼ 4100 $m^2 g^{-1}$; pore volume (V_p) = 2.02 $cm^3 g^{-1}$; pore size of 11.7 and 16 Å) was achieved via visible-light-mediated C−C bond-forming catalysis within photosensitizing porous materials.[58] The process of trapping the guest molecule was accomplished under metal-free and very mild conditions, leading to novel functionalized MOFs with more $\pi-\pi$ stacking, H bonding properties, and outstanding adsorption capacity to eliminate herbicides from the aqueous solutions. The synthesized MOFs removed up to 96.9% of the tested herbicides from the aqueous solutions even at initially very low herbicide concentrations (30 ppm). Particularly, the Br derivative MIL-101(Cr)-C5 inhibited the maximum adsorbed capacities for DUR, alachlor, and tebuthiuron with adsorption capacities of 186.4, 150.2, and 95.2 $mg·g^{-1}$, respectively. Very recently, a composite based on Zr-MOF UiO-66-NH_2 ($[Zr_6O_4(OH)_4(BDC\text{-}NH_2)_6]·nH_2O$; S_{BET} ∼ 950 $m^2 g^{-1}$; pore size of ∼11 and 8 Å; $H_2BDC\text{-}NH_2$: 2-aminoterephthalic acid) was described for the removal of herbicides in water.[59] UiO-66-NH_2 was loaded on the carbon nanotube aerogels (MPCAs) by the *in situ* nucleation and growth of the UiO-66-NH_2 NPs onto the carbon nanotubes (UiO-66-NH_2@MPCA). The study on the adsorption of chipton and alachlor demonstrated that the adsorption capacity of UiO-66-NH_2@

https://doi.org/10.1021/acsami.2c00615
ACS Appl. Mater. Interfaces 2022, 14, 16983−17007

Table 1. Reported MOFs and MOF Composites Related to the Adsorption and/or Degradation of Agrochemicals[a]

agrochemical	MOF/MOF composite	elimination (% or $mg \cdot g^{-1}$)	conditions	reusability (cycles)	ref, year
acetamiprid thiacloprid	$\{Sr^{II}Cu^{II}_6[(S,S)\text{-methox}]_{1.5}[(S,S)\text{-Mecysmox}]_{1.50}(OH)_2(H_2O)\}\cdot 36H_2O$	100%	adsorption, 30 s, 100 ppm, aqueous solution	10	67, 2021
alachlor	Cr-MIL-101-C5 (among others)	186.4 $mg \cdot g^{-1}$	adsorption, 24 h, 30 °C, pH = 3–5, 30 ppm, aqueous solutions		58, 2019
DUR		150.2 $mg \cdot g^{-1}$			
tebuthiuron		95.2 $mg \cdot g^{-1}$			
gramoxone		ca. 60 $mg \cdot g^{-1}$			
ATZ	NU-1000	93%	adsorption, <5 min, 10 ppm, RT, aqueous solutions	3	61, 2019
ATZ	M.MIL-100(Fe)@ZnO	~78%	photodegradation, 1 h, 5 ppm, pH = 2, $+H_2O_2$, 500 W Xe, aqueous solutions	5	68, 2019
ATZ	UiO-67	6.78 $mg \cdot g^{-1}$	adsorption, pH = 6.9, 25 ppm, 2 and 40 min, aqueous solutions	3	69, 2018
	ZIF-8	10.96 $mg \cdot g^{-1}$			
bentazon	MOF-235	7.15 $mg \cdot g^{-1}$	adsorption in aqueous solutions		70, 2015
clopyralid		9.76 $mg \cdot g^{-1}$			
IPU		10.00 $mg \cdot g^{-1}$			
chipton	UiO-66-NH_2@MPCA	227.3 $mg \cdot g^{-1}$	adsorption, 12 h, 10–100 ppm, 30 °C, aqueous solutions	5	59, 2021
chlorantraniliprole	Al-TCPP	371.91 mg g^{-1}	adsorption, 7.5 h, 50 ppm, 25 °C, aqueous solution		71, 2021
chlorpyrifos	MIL-53(Fe)@$AgIO_3$	93–97% (Ad) 70% (Photo)	adsorption, photodegradation, 1 h, solar light, tap water		63, 2018
chlorpyrifos	MIL-53(Fe)@CA	356.34 $mg \cdot g^{-1}$	adsorption, 8 h, 20 ppm, 30 °C, aqueous solution	5	72, 2021
chlorpyrifos malathion methyl	MIL-53(Fe)@$AgIO_3$	78–90%	catalysis, 1 h, solar light, tap water and distilled water		63, 2018
cyhalothrin	ZrO_2@HKUST-1	99.6%	photodegradation, 6 h, 60 $mg \cdot L^{-1}$, 14 W, 25 °C, aqueous solutions	4	73, 2019
2,4-D	MIL-53(Cr)	556 $mg \cdot g^{-1}$	adsorption, 1 h, 100 ppm, RT, aqueous solutions	3	57, 2013
2,4-D	ZIF-8@ionic liquid	448 $mg \cdot g^{-1}$	adsorption, 12 h, 50–200 ppm, pH = 3.5, aqueous solutions		74, 2017
2,4-DP	[Zn(BDC-NH_2)(bpd)]	91%	adsorption, 90 min, 60 ppm, water solutions		75, 2018
2,4-DP	HRP@H-MOF(Zr)	100%	catalysis, 15 min, 6 mM, 25 °C, valley water		65, 2019
2,4-DP	UiO-66-NMe_3^+	279 $mg \cdot g^{-1}$	adsorption, 2 h, 20 ppm, 25 °C, aqueous solutions	7	76, 2020
2,4-DP	ILCS/U-10	262.45 $mg \cdot g^{-1}$	adsorption, 1 h, pH = 2–4, 25–30 °C, aqueous solutions	4	77, 2020
diazinon	MIL-101(Cr)	260.4 $mg \cdot g^{-1}$ 92.5%	adsorption, 3 min, 150 ppm, pH = 7, aqueous solution in continuous flow	4	78, 2018
diazinon	MIP-202/chitosan–alginate beads	17.77 $mg \cdot g^{-1}$	adsorption, 40 min, 50 ppm, pH = 7, 22 °C, aqueous solution	5	79, 2021
diazinon	Bp@MIL-125	96%	photocatalysis, 30 min, 20 ppm, pH = 7, UV lamp, aqueous solution		80, 2021
diazinon	BSA/PCN-222(Fe)	400 $mg \cdot g^{-1}$	adsorption, 3 min, 800 ppm, pH = 7, aqueous solution	12	81, 2021
parathion methyl		370.4 $mg \cdot g^{-1}$			
dichlorvos	UiO-67	571.43 $mg \cdot g^{-1}$	adsorption, 200 min, 25 °C, 200 ppm, pH = 4, aqueous solutions		82, 2019
metrifonate		378.78 $mg \cdot g^{-1}$			
		97.8% and 99%			
dimethoate	Cu-BTC@CA	282.3–321.9 $mg \cdot g^{-1}$	adsorption, 6 h, 30 °C, pH = 7, 20 ppm, aqueous solutions	5	83, 2021
dimethoate	Al-$(BDC)_{0.5}(BDC\text{-}NH_2)_{0.5}$	344.7 $mg \cdot g^{-1}$	adsorption, 8 h, 30 °C, 20 ppm, aqueous solutions		84, 2021
DUR	ZIF-8@ionic liquid	284 $mg \cdot g^{-1}$	adsorption, 12 h, 10–20 ppm, pH = 6.6, aqueous solutions	4	74, 2017
ethion	CuBTC@Cotton	182 $m \cdot g^{-1}$	adsorption, 2 h, aqueous solutions	5	85, 2016
		97%			
ethion	ZIF-8	279.3 $mg \cdot g^{-1}$	adsorption, 8 h, 25 °C, 50 ppm, aqueous solutions	4	86, 2019
	ZIF-67	210.8 $mg \cdot g^{-1}$			
fenamiphos	NU-1000	ca. 6400 $mg \cdot g^{-1}$ (0.89 mol/mol)	adsorption, 2 h, 108.8 ppm, aqueous solution, dynamic conditions	3	87, 2021
fenitrothion	active-extruded-UiO-66	90.2–95.9%	adsorption, 28 ppm, pH = 7, tap and river water		88, 2021

https://doi.org/10.1021/acsami.2c00615
ACS Appl. Mater. Interfaces 2022, 14, 16983–17007

Table 1. continued

agrochemical	MOF/MOF composite	elimination (% or $mg \cdot g^{-1}$)	conditions	reusability (cycles)	ref, year
fipronil and its metabolites	M-ZIF-8@ZIF-67	95%	adsorption, 1 h, 100 ppm, pH = 6, aqueous solutions and cucumber		89, 2020
GLU	NU-1000	186 $mg \cdot g^{-1}$	aqueous solutions		90, 2020
GLY		168 $mg \cdot g^{-1}$			
GLU	UiO-67	360 $mg \cdot g^{-1}$	Adsorption, 300 min, 0.01 mM, 25 °C, pH = 4, aqueous solutions		91, 2015
GLY	NU-1000	1516.02 $mg \cdot g^{-1}$ 100%	adsorption, 20 min, 1.69 ppm, aqueous solutions		60, 2018
GLY	UiO-67	537 $mg \cdot g^{-1}$	adsorption, 300 min, 0.01 mM, 25 °C, pH = 4, aqueous solutions		91, 2015
GLY	UiO-67@GO	483.0 $mg \cdot g^{-1}$	adsorption, 300 min, pH = 4, 40 ppm, aqueous solutions		92, 2017
GLY	MIL-101(Cr)-NH_2	64.25 $mg \cdot g^{-1}$	adsorption, 12 h, 25 °C, pH = 2−4, 100 ppm, aqueous solutions		93, 2018
GLY	Fe_3O_4@SiO_2@UiO-67	256.54 $mg \cdot g^{-1}$	adsorption, 2 h, RT, 20−70 ppm	4	94, 2018
imidacloprid	Bi_2WO_6/MIL-88B(Fe)-NH_2	84%	photocatalysis, 3 h, 10 ppm, pH = 9, Xe lamp	5	95, 2021
IPU	CPO@H-MOF(Zr)	100%	catalysis, 15 min, 20 μM, 25 °C, valley water		65, 2019
mecoprop	UiO-66	51 $mg \cdot g^{-1}$	adsorption, 6 h, 20−170 ppm, 25 °C, pH = 2−5, aqueous solutions	3	96, 2015
mecoprop	Basolite Z1200		adsorption, aqueous solutions		97, 2013
NIT	PCN-224	95%	photodegradation, 20 min, aqueous solution		62, 2020
paraquat	MIL-101(Cr)@α-Fe_2O_3@TiO_2	87.5%	catalysis, 45 min, 20 ppm, pH = 7, 25 °C, aqueous solutions		64, 2018
paraoxon	UiO-66	100%	catalysis, 30 min, RT, 1 mM, pH = 7.8, aqueous solutions		98, 2018
parathion methyl	CuBTC@PAN	90%	adsorption, 2 h, aqueous solutions		99, 2014
propiconazole	MIL-101(Cr)	89.3%	adsorption, 100 min, pH = 3, aqueous solutions	5	100, 2021
prothiofos	ZIF-8 ZIF-67	366.7 $mg \cdot g^{-1}$ 261.1 $mg \cdot g^{-1}$	adsorption, 8 h, 25 °C, 50 ppm, aqueous solutions	4	86, 2019
QPE	QpeH@ZIF-10	88%	enzymatic degradation, 14 days, pH = 6.7, watermelon field	10	66, 2021
thiamethoxam	MIL-100(Fe)@Fe-SPC	95.4%	catalysis, 180 min, 60 ppm, pH = 7.5, 25 °C, +H_2O_2, us	5	101, 2018
NND	M-MOF	1.8−3.0 $mg \cdot g^{-1}$	adsorption, 1 h, 100 ppm, aqueous mixture of contaminants		102, 2017
OP	ZIF-8@M-M	96%	adsorption, 15 min, 0.2−8 ppm, pH = 2−10, aqueous mixture of contaminants	5	103, 2018

[a]The table is sorted according to the studied agrochemical, followed by the MOF-based material name (or chemical formula), elimination capacity (% or $mg \cdot g^{-1}$), optimal conditions for the elimination (mechanism, time to reach the equilibrium, concentration of the agrochemical, temperature, pH, type of light, and other species involved during the catalytic process), and cycles of reuse. Bp: black phosphorus; bpd: 1,4-bis(4-pyridyl)-2,3-diaza-1,3-butadiene; BSA: bovine serum albumin; CA: cellulose acetate; Fe-SPC: Fe-doped nanospongy porous biocarbon; GO: graphene oxide; H_2BDC-NH_2: 2-aminoterephthalic acid; HRP: horseradish peroxidase; H_3BTC: 1,3,5-benzenetricarboxylic acid; ILCS: ionic liquid modified chitosan; M-M: magnetic multiwalled carbon nanotubes; MPCAs: carbon nanotube aerogels; PAN: polyacrylonitrine; QpeH: quizolafop-P-ethyl hydrolase esterase; RT: room temperature; us: ultrasound.

MPCA was improved with respect the single MOF NPs, which is indicative of a synergistic effect between the MOF and MPCA (i.e., the chipton adsorption capacity is improved from 98.4 to 227.3 $mg \cdot g^{-1}$ for UiO-66-NH_2 and UiO-66-NH_2@MPCA, respectively). Further, rice was used to assess the biosecurity of the composite. Remarkably, UiO-66-NH_2@MPCA could reduce the accumulation of Zr^{4+} in the roots and leaves of rice in comparison with the UiO-66-NH_2 NPs, demonstrating that MPCA can diminish the potential environmental risk of the MOF materials. Lastly, the authors demonstrated the reusability of the composite up to 5 times without decreasing its adsorption capacity. Finally, we want to highlight two reports utilizing the water stable Zr-based MOF NU-1000 ($[Zr_6(\mu_3\text{-}O)_4(\mu_3\text{-}OH)_4(-OH)_4(-OH_2)_4(PyTBA)_2]$; PyTBA: 4,4′,4″,4‴-(pyrene-1,3,6,8-tetrayl)tetrabenzoate; $S_{BET} \sim 2100\ m^2 \cdot g^{-1}$; pore size of ∼12 and 30 Å). In the first study, reported by Pankajakshan et al.,[60] NU-1000 was described for the efficient elimination of GLY from aqueous media. NU-1000 comprises $[Zr_6(\mu_3\text{-}O)_4(\mu_3\text{-}OH)_4(H_2O)_4(OH)_4]$ as secondary building units, acting as Lewis acid nodes that can react with the Lewis base phosphate group of GLY. Theoretical calculations demonstrated that the interaction energy of GLY with the NU-1000 nodes was $-37.63\ KJ \cdot mol^{-1}$. NU-1000 was synthesized in different particle size scales (100−2000 nm), reducing the equilibrium times with smaller MOF sizes and

https://doi.org/10.1021/acsami.2c00615
ACS Appl. Mater. Interfaces 2022, 14, 16983−17007

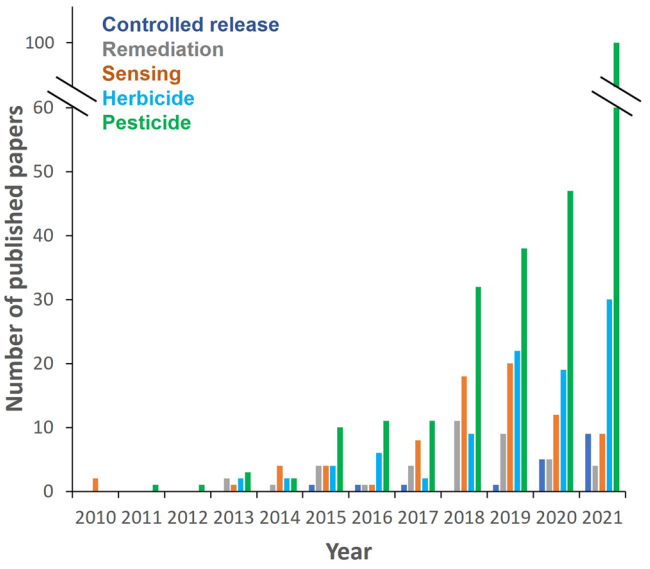

Figure 3. Number of published papers having keywords MOF and agriculture in their titles and abstracts, separated by areas (i.e., controlled release, remediation, and sensing) and important related words (herbicide and pesticide). Retrieved from the Web of Science on March 10, 2022.

achieving a total GLY loading of 1516.02 mg·g^{-1} (or 8.97 mg·g^{-1}) in only 20 min. In the second work, the same authors thoroughly investigated the mechanism governing ATZ adsorption on Zr_6-based MOFs (UiO-66-X, where X = H, OH, NH_2; DUT-52; UiO-67; NU-901; NU-1000; and NU-1008) by investigating the impact of MOF used linkers and topology on ATZ uptake capacity and kinetics.[61] Among all the tested Zr-MOFs, it was found that the mesopores of NU-1000 facilitate the rapid ATZ uptake, saturating in less than 5 min. Excluding the pyrene-based linker, NU-1008 ($[Zr_6(\mu\text{-}O)_4(\mu\text{-}OH)_4(HCOO)(H_2O)_3(OH)_3(TCPB)_2]$; TCPB: 1,2,4,5-tetrakis(4-carboxyphenyl)benzene; S_{BET} ~ 1400 m^2·g^{-1}; pore size of ~14 and 30 Å) removed <20% of the exposed ATZ. The pyrene-based linker seems to offer enough sites for $\pi-\pi$ interactions with ATZ as revealed by the near 100% uptake (Figure 4). These results indicate that the ATZ uptake in NU-1000 stems from the existence of a pyrene core in the linker of the MOF, which confirms that the $\pi-\pi$ stacking is the main force of the ATZ adsorption. Finally, the cyclability of the MOF was demonstrated through 3 adsorption−desorption cycles.

4.2. Catalytic Processes. The number of studies related to the catalytic degradation of agrochemicals using MOFs or MOF composites are very limited. The literature mainly focuses on the use of MOF composites with only one work based on a simple MOF. This study describes the bifunctional nanoscale porphyrinic MOF PCN-224 (or $[Zr_6(TCPP)_{1.5}]$; H_2TCPP: tetrakis(4-carboxyphenyl)porphyric; S_{BET} = 2600 m^2·g^{-1}; V_p = 0.95 cm^3·g^{-1}; pore size = 1.9 nm) as both the sensor for the recognition of trace NIT and the photocatalyst to enable the pesticide degradation.[62] The intense fluorescence of the probe was quenched by NIT, leading to a sensing range from 0.05 to 10.0 μg·mL^{-1}. The potentiality of PCN-224 in the degradation of NIT was further identified. The photodegradative effectiveness was up to 95% after only 20 min of laser irradiation, whereas no significant NIT degradation was detected under darkness, regardless of the PCN-224 presence. Therefore, this material could be established as an all-in-one nanoplatform for pesticide sensing, detection, and posterior photodegradation in agricultural farmland and other environments. Among other MOF-based composites, metallic NP composites are the most employed. The MIL-53(Fe)@$AgIO_3$ composite was successfully applied in the decomposition of two organophosphate pesticides (OPs; malathion methyl and chlorpyrifos) under sunlight irradiation.[63] After 1 h of solar light irradiation, 78−90% of both pesticides was individually degraded in tap and distilled water. In binary mixtures (both composites), 70% of mineralization is achieved after 3 h. Another example of metallic NPs@MOF composites is magnetic α-Fe_2O_3@MIL-101(Cr)@TiO_2 for the degradation of paraquat herbicide from aqueous solution.[64] A maximum photocatalytic degradation was achieved at optimal conditions (see Table 1; 87.5% after 45 min), demonstrating the utility of

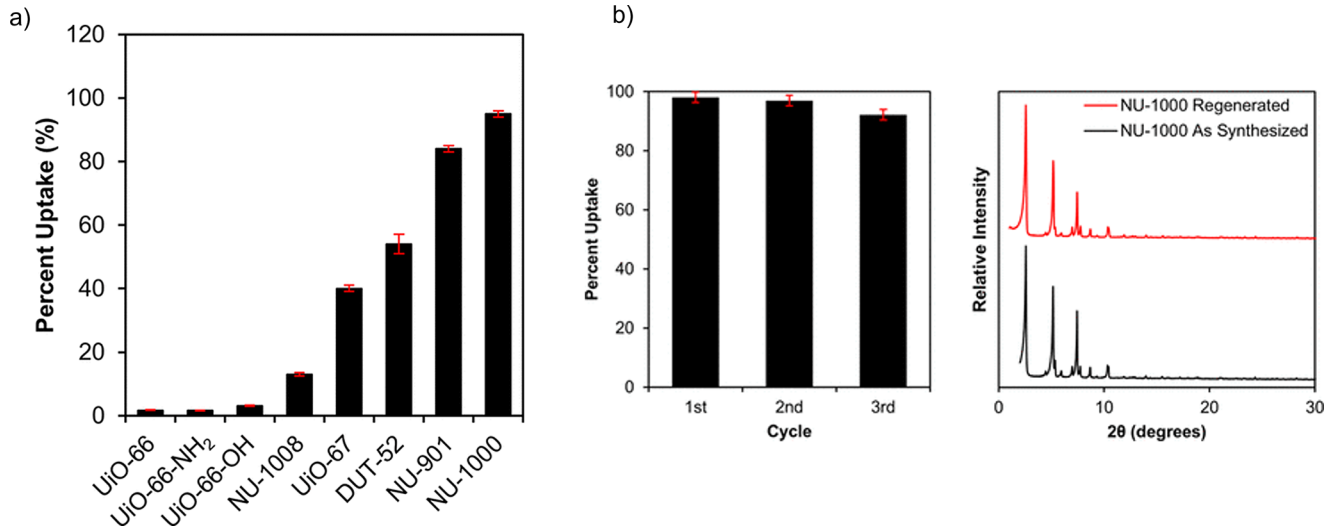

Figure 4. (a) ATZ uptake as a percentage of the total amount of ATZ exposed to Zr-MOFs for 24 h and (b) through 3 cycles of ATZ adsorption and regeneration with acetone using NU-1000 while maintaining its crystallinity. Reprinted from ref 61. Copyright 2019 American Chemical Society.

https://doi.org/10.1021/acsami.2c00615
ACS Appl. Mater. Interfaces 2022, 14, 16983−17007

Table 2. Previously Reported MOF-Based Materials Associated with the Controlled Release of Agrochemicals[a]

agrochemical	MOF/MOF composite	loading (wt % or mmol·g^{-1})	release conditions	activity studies	ref, year
azoxystrobin	MIL-100(Fe)	16.2 wt %	80% (pH = 5.0), 85% (pH = 7.2), 86% (pH = 8.5) with PBS, ethanol, and Tween-80 emulsifier	fungicidal activity against (*Fusarium graminearum* and *Phytophthora infestans*) 5 and 15 ppm, 56% and 62% of inhibition in 7 days, nutritional function of Fe	109, 2020
azoxystrobin; diniconazole	MIL-101(Al)-NH_2	6.71%; 29.72%	90% in 46 and 136 h	germicidal efficacy against rice sheath blight (*Rhizoctonia solani*), EC_{50} = 0.065 mg·mL^{-1}	110, 2021
λ-cyhalothrin	UiO-66	87.71 wt %	70% in 12 h in DMF or 60% DMF aqueous solution	insecticide activity assay (*Musca domestica*) KT_{50} = 3.64, 5.12, and 6.91 min after being treated 1, 15, and 30 days; bioactivity (*Aphis craccivora*) LC_{50} = 3.20, 0.70, and 0.36 ppm at 24, 48, and 72 h	111, 2020
1,3-DCPP	MOF-1201; MOF-1203	1.4 mmol·g^{-1}; 13 wt %	80% in 100 000 min·g^{-1} under air flow 1.0 cm^3·min^{-1}		105, 2017
chlorantraniliprole	MIL-101(Fe)@silica	23%	dialysis method, water, sink conditions	photostability improvement (16.5 times more stable), insecticidal activity against *Plutella xylostella* (LC_{50} = 0.389 mg·L^{-1})	112, 2021
diniconazole	PDA@NH_2-Fe-MIL-101	28.1 wt %	PBS/ethanol/Tween-80 emulsifier	fungicidal activity against *Fusarium graminearum* 1 and 5 ppm for 4 days of inhibition of 44% and 86%	113, 2020
dinotefuran	MIL-101(Fe)@CMCS	24.5%	83.1% aqueous solution stimulated by citric acid in ca. 18 h	photostable (70%) after 48 h of irradiation, insecticidal activity in soil	114, 2020
dinotefuran, Zn^{2+}	PFAC	13.60%	photothermal triggered release (49% at 40 °C), pH response release (pH = 4.0 and 7.0 is 52.63% and 31.87%)	stem length (39.2 vs 33.9 cm) and root length (19.7 vs 13.5 cm) of the corn were clearly improved after 25 days of cultivation	115, 2021
gibberellin	CLT6@PCN-Q	0.78 mmol g^{-1}	release under stimuli (pH, temperature, and competitive agent)	germination of Chinese cabbages and monocotyledonous wheat	116, 2021
imidacloprid	Fe_3O_4@PDA@UiO-66	15.87%	dialysis method in water (50% in 48 h)	insecticidal activity against *Aphis craccivora* Koch (LC_{50} = 2.15 mg·L^{-1}, comparable to the commercialized formulation)	117, 2021
NH_4^+	MOF(Fe)@NaAlg(2:10)	1.63 mmol·g^{-1}	release in water (80%) and soil (69%) in 28 days	water retention of soil	118, 2020
ortho-disulfides (DiS-NH_2 and DiS-*O*-acetyl)	ZIF-8	42.8 and 16.71 wt %	ca. 85% in 2 h of PBS (pH = 5.5)	IC_{50} = 5.413 and 3.892 μM, phytotoxicity bioassay against *Echinochloa crusgalli*, *Amaranthus viridis*, and *Lollium rigidum*	119, 2021
oxalate; urea	OPA-MOF	3.1% of N; 12.5% of P, 14.5% of oxalate		soil incubation and crop growth (wheat)	56, 2015
oxalate; urea	OPA-MOF I and II	3.2% and 5.8% of N; 11.3% and 15.6% of P			104, 2016
prochloraz	PD@ZIF-8		pH and light response, release in dark (13.7%) vs light (63.4%)	cytotoxicity under light EC_{50} = 0.122 μg·mL^{-1}, fungal activity (*Sclerotinia sclerotiorum*), updated in plants (oilseed rape)	120, 2021
tebuconazole	MIL-101(Fe)-TA	24.1 wt %	stimuli response (pH, sunlight, H_2O_2, GSH, PO_4^{3-}, and EDTA)	cytotoxicity (HLF-1), safety (wheat seedlings), and fungicidal activity (*Rhizoctonia solani* and *Fusarium graminearum*)	107, 2021
tebuconazole	PCN-224@P@C	30 wt %	174 h in PBS solution (pH = 5) 17.2%, stimuli response to pectinase in PBS (pH = 5) 86.9% in 174 h	fungicidal activity (*Xanthomonas campestris* pv *campestris*, *Pseudomonas syringae* pv *tomato*, and *Alternaria alternate*) and safety (Chinese cabbage)	106, 2019
thiamethoxam	UiO-66-NH_2/SL	33.56 wt %	PBS solution at 37 °C (ca. 80% in 60 h), soil column (76.8% in 48 days)	biosafety (100% rice seed germination)	121, 2021
TMPyP	HKUST-1		light irradiation (day/night temperature was 25/18 °C, photoperiod was 15/9 h, and the humidity was at 60−80% (irradiance of 9 mW cm^{-2} and energy of 3.18 kJ cm^{-2})	photodynamic fungicidal activity (*P. syringae pv lachrymans* and *C. michiganense* subsp. *Michiganense*), efficacy (*Sclerotinia sclerotiorum*), and safety to plants (cucumber and Chinese cabbage)	108, 2021

[a]The table is organized according to the agrochemical, followed by the MOF-based material name (or chemical formula), loading capacity (wt % or mmol·g^{-1}), release conditions, and activity tests. C: chitosan; CMCS: carboxymethyl chitosan; DMF: *N*,*N*′-dimethylformamide; EDTA: ethylenediaminetetraacetate; GSH: glutathione; HLF-1: human lung fibroblast; IC_{50}: half maximal inhibitory concentration; KT_{50}: 50% knockdown time; LC_{50}: median lethal concentration; OPA: oxalate-phosphate-amine; P: pectin; PBS: phosphate buffer saline; PD: prochloraz (P) and 2,4-dinitrobenzaldehyde (D); PDA: polydopamine; SL: sodium lignosulfonate; TA: tannic acid; TMPyP: 5,10,15,20-tetrakis(1-methyl-4-pyridinio)porphyrin tetra(*p*-toluenesulfonate).

https://doi.org/10.1021/acsami.2c00615
ACS Appl. Mater. Interfaces 2022, 14, 16983−17007

these systems in the photocatalytic degradation of agrochemicals in water.

MOFs have also been used as support for the stabilization of enzymes able to degrade agrochemicals in wastewater and soil. Gao et al. described the preparation of a hierarchically porous MOF (H-MOF(Zr)) as support of the chloroperoxidase (CPO) and horseradish peroxidase (HRP) enzymes, leading to the CPO/HRP@H-MOF(Zr) composite.[63] CPO@H-MOF(Zr) and HRP@H-MOF(Zr) composites were applied in the treatment of wastewater containing IPU and 2,4-D, achieving a complete and very fast (15 min) degradation. Finally, we want to highlight the fabrication of purified esterase embedded in zeolitic imidazolate frameworks (ZIFs) for the degradation of pesticides.[66] Particularly, in this work, aryloxyphenoxypropionate herbicide-hydrolyzing enzyme, QpeH, was embedded into ZIF-10 ($[Zn(Im)_2]$; Im: imidazonate) and ZIF-8 ($[Zn(Hmim)_2]$; Hmim: 2-methylimidazole; $S_{BET} \sim 1260\ m^2\ g^{-1}$, $V_p \sim 0.6\ cm^3\ g^{-1}$, pore size of ~3.4 and 11.4 Å) and tested in the degradation of quizalofop-P-ethyl in a watermelon field. Remarkably, the QpeH@ZIF-10 composite showed a slightly improved degradation efficiency compared to QpeH@ZIF-8 (88% vs 84%). Unfortunately, no ZIF degradation studies were performed in this research in an attempt to rationalize the different behaviors of both ZIF composites and their potential application in real water treatments. It should be noted that the QpeH@ZIF composites were demonstrated to affect the recovery of the bacterial community in soil.

5. MOFs AS AGROCHEMICAL DELIVERY AGENTS

The recent enthusiasm around the use of MOFs as agrochemical delivery agents is highlighted in Figure 3 with a significant increase in the number of papers published on the topic in the last two years. All the studies reported so far on the controlled release of agrochemicals from MOFs are summarized in Table 2, again sorted by the different types of released agrochemical: (i) **herbicides**, *cis*-1,3-dichloropropene (1,3-DCPP) and ortho-disulfides; (ii) **fungicides**, diniconazole, prochloraz, tebuconazole, and zoxystrobin; (iii) **insecticides**, chlorantraniliprole, λ-cyhalothrin, dinotefuran, imidacloprid, and thiamethoxam; (iv) **fertilizers**: urea; (v) **plant grow regulators**: gibberellin. The first MOF described as a delivery agent of agrochemicals was OPA-MOF (OPA: oxalate−phosphate−amine). In 2015, Anstoetz et al. described the use of an OPA-MOF as a microbially induced slow-release N and P fertilizer.[56] In this research, the capacity of the urea-templated OPA-MOF as a new fertilizer with a slow release was investigated and compared with a standard P (triple superphosphate) and N (urea) fertilizer (ferralsol). The authors hypothesize that the OPA-MOF is a gradual-release fertilizer for crops grown on acidic soils, where microbial consumption of the oxalate linker gives rise to the degradation of the framework structure, thereby releasing Fe phosphate. While in the OPA-MOF treatment the hydrolysis of urea was fast, the conversion of the ammonium to nitrate was significantly diminished in comparison with the urea treatment (ferralsol). However, P uptake and yield in OPA-MOF was considerably lower than in conventionally fertilized plants. OPA-MOF was proven to have potential as an enhanced efficiency N fertilizer but not in P bioavailability. A year later, two novel OPA-MOFs were hydrothermally synthesized and fully characterized to be used again as slow-release fertilizers.[104] The framework backbone is robust and based on FeO_6 units with bidentate oxalate bridges joining adjacent Fe centers. PO_4 units have corner-sharing for all of their oxygens with the FeO_6 units. The authors studied the release of oxalate, setting it high enough to permit oxalate concentrations in the soil solution to achieve 1 $mg{\cdot}L^{-1}$ but also low enough to avoid fast and purely chemically driven compound degradation. The results show that, from the two synthesized materials, OPA-MOF-I has a slow solubility with an oxalate concentration of ca. 5 $mg{\cdot}L^{-1}$ at high loading and seems to be compatible with trials as a fertilizer in future works.

In 2017, Yaghi and co-workers described a naturally degradable MOF as a carrier of the important fumigant *cis*-1,3-dichlorophropene (1,3-DCPP).[105] The MOF $[Ca_{14}(L\text{-lactate})_{20}(acetate)_8X]$ (X: C_2H_5OH, H_2O, or MOF-1201), constructed from Ca^{2+} ions and L-lactate, presents apertures and an internal diameter of 7.8 and 9.6 Å, respectively, and a permanent porosity of 430 $m^2{\cdot}g^{-1}$. MOF-1201 can efficiently encapsulate the 1,3-DCPP agrochemical with a total pesticide loading of 1.4 $mmol{\cdot}g^{-1}$ (13 wt %). Originally, the fumigant release study was performed using an air flow, demonstrating a slow release when purging samples of the 1,3-DCPP loaded MOF (1,3-DCPP@MOF-1201) in an air flow of 1.0 $cm^3{\cdot}min^{-1}$. The loaded 1,3-DCPP@MOF-1201 showed a 100 times slower release compared to that of the liquid 1,3-DCPP, achieving 80% of the total release in 100 000 $min{\cdot}g^{-1}$. Porphyrinic MOFs have also been described as promising carriers of fungicides.[106] Particularly, PCN-224 was loaded (30 wt %) with tebuconazole and constructed layer by layer with chitosan and pectin to get tebuconazole microcapsules. The synthesized microcapsules (Tebuc@PCN@P@C) had a dual-microbial effect on plant bacterial and fungal diseases (Figure 5). First, the tebuconazole previously loaded in the micro-

Figure 5. Mechanism of triggered tebuconazole release and the illustration of the dual-microbicidal effect of the Tebuc@PCN@P@C microcapsules. Reprinted from ref 106. Copyright 2021 American Chemical Society.

capsules was gradually released (87% in 7.25 days) after the pectin layer was decomposed by the pectinase released by the invading pathogen. Second, the singlet oxygen ($^1O_2$) was released from the organic linker porphyrin when the MOF NPs were exposed to light after the formation of pectin to inhibit the pathogens. The synthesized compound displayed excellent double activities of having photodynamic therapy and being

https://doi.org/10.1021/acsami.2c00615
ACS Appl. Mater. Interfaces 2022, 14, 16983−17007

microbicidal against the bacteria *X. campestris* pv *campestris* (82.4% and 18.4% under light and dark, respectively) and *P. syringae* pv *tomato* (56.3% and 9.5% under light and dark, respectively) and the fungi *A. alternate* (68.0%). Finally, the authors studied the safety of this compound against Chinese cabbage (*Brassica rapa pekinensis*) in a greenhouse environment. The results demonstrated that the synthesized microcapsules do not have a major effect on both the fresh weight and the soil plant analysis development (SPAD) value of the tested plant leaf, so the Tebuc@PCN@P@C microcapsules can be considered safe.

A very recent and complete study described a further example of a tebuconazole loaded MOF, the MIL-101(Fe) gated with Fe^{III}-tannic acid (TA) networks.[107] The Fe^{III}-TA complexes are able to absorb UV−vis near-infrared (NIR) lights. The design of MIL-101(Fe)-TA NPs enables the release of the tebuconazole cargo (24.1 wt %) in response to 7 stimuli (i.e., acidic pH, alkaline pH, H_2O_2, glutathione (GSH), phosphate, ethylenediaminetetraacetate (EDTA), and sunlight) to meet the diverse controlled release of the encapsulated cargo (Figure 6). Tebuconazole is gradually

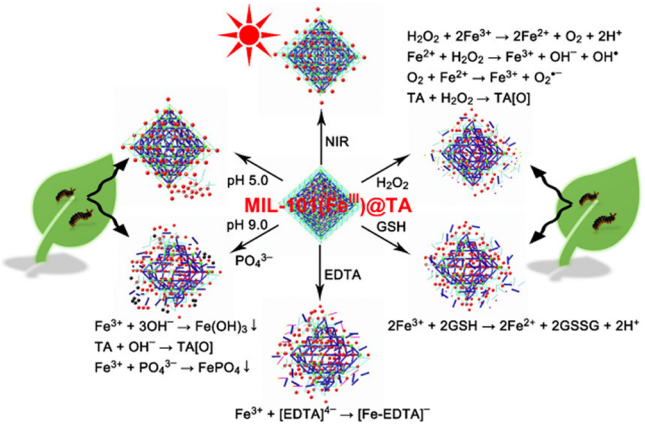

Figure 6. Stimuli-responsive controlled release in MIL-101(Fe^{III}) nanopesticides gated with Fe^{III}-TA networks related to the biological and natural environments of crops and stimuli-responsive mechanisms. TA[O] represents the oxidation product of TA. Reprinted with permission from ref 107. Copyright 2020 Elsevier Inc.

released from the gated MIL-101(Fe) when the pH decreases to 5.0 as a result of the partial disassembly of Fe^{III}-TA networks, and a significant delivery of the pesticide occurred when the pH increases to 9.0 owing to both the disassembly of the Fe^{III}-TA networks and the degradation of the MIL-101(Fe). This is important since, in various parts of the plants themselves or caused by pest and pathogens, there are different pH values. Further, when crop plants suffer from biotic or abiotic stress, H_2O_2 is rapidly produced in cells. On the basis of the Fenton reaction between H_2O_2 and Fe^{II}/Fe^{III}, the release of the cargo will be induced by the degradation of MIL-101(Fe). GSH, normally found in plants and animals, is able to reduce Fe^{III} to Fe^{II}, causing the degradation of MIL-101(Fe) and, then, promoting the release of the encapsulated pesticide. Additionally, phosphates can induce MIL-101(Fe) degradation by competitive coordination with Fe^{III}, and finally, the Fe^{III}-TA networks on MIL-101(Fe) will stimulate the controlled release of the pesticide via the photothermal effect of the NIR light of sunlight. Lastly, this system demonstrated high fungicidal activities against *R. solani* (rice sheath blight; concentration for 50% of the maximal effect, ED_{50}: 0.4960 mg·L^{-1} after 48 h) and *F. gaminearum* (wheat head blight; ED_{50}: 0.5658 mg·L^{-1} after 48 h); good safety in seed germination, seedling emergence, and plant height of wheat by seed dressing; satisfactory control efficacies on wheat powdery mildew caused by *B. graminis*.

Finally, we want to mention a report on the construction of a porphyrin MOF nanocomposite constructed by incorporating 5,10,15,20-tetrakis(1-methyl-4-pyridinio)porphyrin tetra(*p*-toluenesulfonate) (TMPyP) as a photosensitizer (PS) in the cage of HKUST-1 (or CuBTC, $[Cu_3(btc)_2(H_2O)_3]$) (HKUST: Hong Kong University of Science and Technology, $S_{BET} \sim 1300-1600$, $V_p \sim 0.71$ $cm^3 \cdot g^{-1}$) to efficiently produce singlet oxygen to inactivate plant pathogens under light irradiation.[108] The prepared PS@HKUST-1 loaded about 12 wt % of PS, exhibiting an excellent and broad-spectrum photodynamic antimicrobial activity *in vitro* against three plant pathogenic fungi (*S. sclerotiorum*, *P. aphanidermatum*, and *B. cinerea* with >80%, 60%, and 80% efficiency at concentrations of 200, 50, and 200 mg·L^{-1}, respectively) and two pathogenic bacteria (*P. syringae* pv *lachrymans* and *C. michiganense* subsp. *Michiganense*). Besides, *Allium cepa* chromosome aberration assays confirmed that PS@HKUST-1 showed no genotoxicity and safety to the growth of cucumber and Chinese cabbage.

Thus, considering all the mentioned examples, the controlled release of agrochemicals from MOFs and MOF composites is an emerging research field that has demonstrated a great potential as an alternative and efficient new strategy to release plant nutrients but also control pests in agricultural applications.

6. MOFs AS SENSORS OF AGROCHEMICALS

Considering the important detrimental effect of pesticides on human health, researchers have extensively studied and discussed the pretreatment, extraction, detection, and determination of agrochemical residues in water, fruits, and vegetables. These data have been valuable to food analysts and regulatory authorities for monitoring the quality and safety of fresh food products, among others. As would be expected, MOFs and MOF composites have been extensively proposed for the extraction and determination of these dangerous substances in food and water. Many different agrochemicals have been analyzed using MOFs: (i) **herbicides**, ametryn, amidosulfuron, ATZ, atraton, bensulfuron methyl, bis(*p*-nitrophenyl) phosphate, butachlor, carbaryl, chlorimuron ethyl, 2,4-dichlorophenol, 4-chlorophenoxyacetic acid (4-CPA), chlortoluron, 2,4-D, dicamba, desmetryn,2-(2,4-dichlorophenoxy)propionic acid (2-DPP), chlorotoluron, dipropetryn, epoxide, fenuron, fluometuron, glufosinate, GLY, heptachlor prometryn, MCPA, (2-methyl-4-chlorophenoxy) butyric acid (MCPB), (2-methyl-4-chlorophenoxy) propionic acid (MCPP), metsulfuron methyl, monuron, nicosulfuron, metazachlor, molinate, nitrofen, paraquat, pretilachlor, prometon, propanil, pyrazosulfuron ethyl, secbumeton, simazine, sulfometuron methyl, sulfosulfuron, terbumeton, terbuthylazine, thifensulfuron methyl, trietazine, and trifluralin; (ii) **fungicides**: bromuconazole, carbendazim, chlorothalonil, 2,6-dichloro-4-nitroaniline (2,6-DN), difenoconazole, diniconazole, epoxiconazole, fenbuconazole, flusilazole, flutriafol, hexachlorobenzene, hexaconazole, iprodione, myclobutanil, penconazole, prochloraz, propiconazole, pyraclostrobin, pyrimethanil, tebuconazole, thiabendazole, thiophanate methyl,

https://doi.org/10.1021/acsami.2c00615
ACS Appl. Mater. Interfaces 2022, 14, 16983−17007

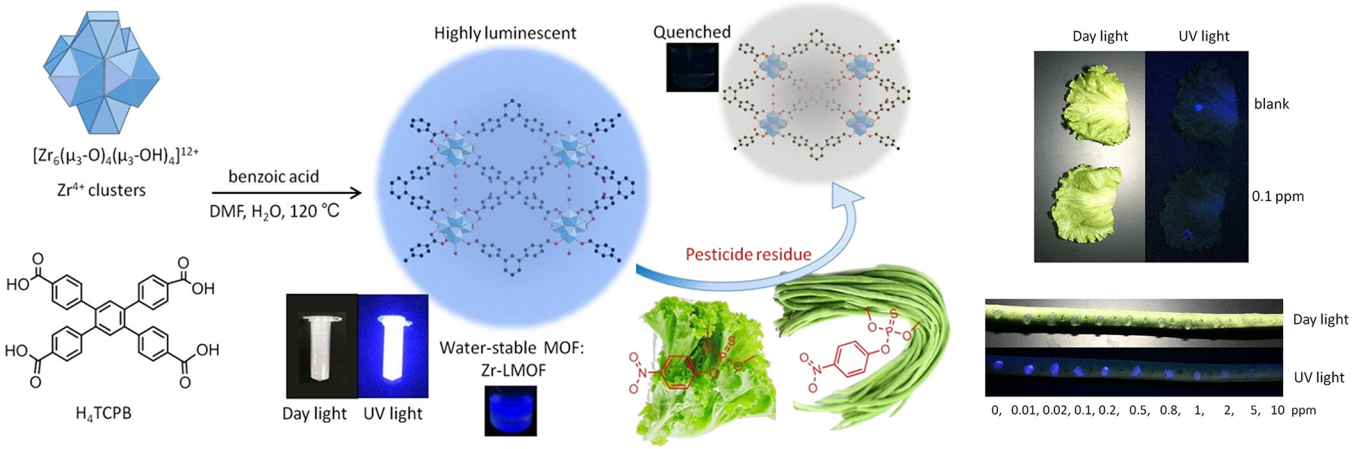

Figure 7. Schematic diagram of the synthesis of CAU-24 and its application for OP pesticide sensing. Insets show the blue fluorescence of the aqueous solution of this Zr-MOF before and after quenching by target parathion methyl in an aqueous solution and directly applied on the surface of vegetable surfaces. Reprinted with permission from ref 125. Copyright 2014 Elsevier B.V.

and triadimefon; (iii) **insecticides**: aldrin, avermectin, azinphos methyl, bifenthrin, bromopropylate, carbofuran, chlordane, chlorfluazuron, chlorpyrifos, clethodim, clofentezine, coumaphos, β-cyfluthrin, cyhalothrin, cyphenothrin, deltamethrin, diazinon, *o,p′*- and *p,p′*-1,1-dichloro-2,2-bis(*p*-chlorophenyl)ethylene (DDE), *p,p′*-1,1-dichloro-2,2-bis(*p*-chlorophenyl)ethylene (*p,p′*-DDD), dichlorvos, dieldrin, difenoxuron, diflubenzuron, dimethoate, diniconazole, dinotefuran, α- and β-endosulfan, fenitrothion, fenpropathrin, fenthion, fenvalerate, flufenoxuron flumetralin, α-, β-, γ-, and δ-hexachlorocyclohexane (HCH), hexaflumuron, imidacloprid, isocarbophos, lufenuron, malathion (also named carbophos), monocrotophos, NIT, nitenpyram, *p*-nitrophenyl phosphate, matrine, methamidophos, paraoxon, paraoxon ethyl, parathion, parathion methyl, penfluoron, permethrin, phosalone, pirimiphos, procymidone, profenofos, pyridaben, pyrimicarb, quinalphos, teflubenzuron, triazophos, thiamethoxam, tribenuron methyl, trichlorfon, *o,p′*- and *p,p′*-1,1,1-trichloro-2,2-bis(*p*-chlorophenyl)ethylene (DDT), 1,1,1-trichloro-2,2-bis-(4chlorophenyl)ethane, triflumuron, and thiacloprid; (iv) **plant growth hormones**: forchlorfenuron, 6-benzylaminopurin, indole-3-acetic acid, 3-indolebutyric acid, and indolepropionic acid.

In 2010, Wen et al. reported one of the first works about the application of MOFs in the efficient detection of agrochemicals. In this study, a new MOF, named $[Cd(2,2',4,4'\text{-bptcH}_2)]_n$ (2,2′,4,4′-bptcH$_4$: 2,2′,4,4′-biphenyltetracarboxylic acid), that was thermally stable and luminescent was prepared via a hydrothermal reaction.[122] This material was tested as a solid-phase extraction (SPE) material for the detection of trace levels of organophosphate pesticide (OP) via stripping voltametric analysis. The determination of parathion methyl as a model included two main steps: parathion methyl adsorption and electrochemical stripping detection of adsorbed pesticide. The MOF modified glass carbon electrode was immersed into a sample solution containing the desired parathion methyl concentration, and the peak currents increased rapidly with the immersion time, up to 12 min, which indicated the saturation. The calculated limit of detection (LOD: 0.0006 $\mu g \cdot mL^{-1}$) is comparable with that of 0.0048 $\mu g \cdot mL^{-1}$ at a hanging mercury drop electrode, suggesting that the reported MOF is reliable for the determination of OPs in water. The same year, Barreto et al. reported the evaluation a new adsorbent 3D MOF $[(La_{0.9}Eu_{0.1})_2(DPA)_3(H_2O)_3]$ (H_2DPA: pyridine-2,6-dicarboxylic acid) for the determination of pesticides from four chemical classes, namely, organochlorine (endosulfan), organophosphate (malathion and parathion methyl), dicarboximide (procymidone), and carbamate (pirimicarb) in fresh lettuce (*Lactuca sativa*) by matrix solid-phase dispersion (MSPD) and gas chromatography−mass spectrometry (GC/MS).[123] The recoveries obtained ranged from 78% to 107% with relative standard deviation (RSD) values between 1.6% and 8.0%. The LOD and limit of quantification (LOQ) ranged from 0.02 to 0.05 $mg \cdot kg^{-1}$ and from 0.05 to 0.1 $mg \cdot kg^{-1}$, respectively, for the different pesticides studied. Importantly, the comparison with a conventional sorbent (silica gel) showed better performance of the MOF sorbent for all tested pesticides. However, the reasons of this improvement are not investigated or discussed by authors. Later on, in 2017, Tao et al.[124] originally synthesized a tetraphenylethene-based ligand (BPyTPE: (*E*)-1,2-diphenyl-1,2-bis(4-(pyridin-4-yl)phenyl)-ethene) with a *trans* conformation and prominent AIE properties. On the basis of BPyTPE, a novel 2D pillared-layered LMOF $[Zn_2(bpdc)_2(BPyTPE)]$ (H_2bpdc: biphenyl-4,40-dicarboxylic acid) was developed showing a 3-fold interpenetration structure. The activated material (without solve) exhibits a strong blue-green emission at 498 nm with an important φ_F of 99%. The emission of the MOF without solvent can be quenched selectively and effectively by 2,6-DN. Thus, the authors established a method to quantitatively and sensitivity detect trace 2,6-DN with a linear range of 0.94−16.92 ppm and a low detection limit of 0.13 ppm.

When one considers these outstanding original works, MOFs have opened a new opportunity for the development of efficient techniques to detect agrochemicals. However, most of these materials are more or less sensitive to moisture or water and can be degraded through hydrolysis. Only few MOFs can maintain their stability in water or a moist environment. One example is the previously reported luminescent Zr-MOF CAU-24, based on the C-centered orthorhombic arrangement cluster $[Zr_6(\mu_3\text{-}O)_4(\mu_3\text{-}OH)_4^{12+}]$ bridged by $TCPB^{4-}$ linkers in a scu topology (H_4TCPB: 1,2,4,5-tetrakis(4-carboxyphenyl)benzene; S_{BET}: 1450 $m^2 \cdot g^{-1}$; rhombic channels of ~10 × 5.3 and ~3.5 × 2.4 Å^2, Figure 7). This material demonstrated a rapid, sensitive, and *in situ*

https://doi.org/10.1021/acsami.2c00615
ACS Appl. Mater. Interfaces 2022, 14, 16983−17007

Table 3. Reported MOFs and MOF Composites Related to the Detection of Agrochemicals[a]

agrochemical	MOF/MOF composite	recovery (%)	applicability	detection limit	ref, year
aldrin	MOF-199/GO fiber	90.6−104.4	river water	$2.3-6.9 \times 10^{-3}$ ppm	130, 2013
chlordane		82.7−96.8	soil		
p,p′-DDE		72.2−107.7	water convolvulus		
p,p′-DDD		82.8−94.3	longan		
dieldrin					
endosulfan					
heptachlor epoxide					
hexachlorobenzene					
aldrin	needle trap device packed with the MIL-100(Fe)		air environment	0.04−0.41 $\mu g \cdot m^{-3}$	131, 2021
chlordane					
dieldrin					
o,p′-DDT					
p,p′-DDT					
hexachlorobenzene					
1,1,1-trichloro-2,2-bis(4chlorophenyl) ethane					
ametryn	MIL-101(Cr)	73.37−107.7 ± 0.10−14.58	corn	0.01−0.12 $ng \cdot g^{-1}$	132, 2018
atraton					
desmetryn					
dipropetryn					
prometon					
prometryn					
ametryn	MIL-101(Cr)	91.1−106.7	soybean	1.56−2.00 $\mu g \cdot kg^{-1}$	133, 2015
atraton					
atz					
chlorotoluron					
fenuron					
monuron					
terbuthylazine					
ametryn	MIL-101(Cr)	89.5−102.7	peanuts	0.98−1.9 $\mu g \cdot kg^{-1}$	134, 2014
atraton					
ATZ					
chlortoluron					
monuron					
terbumeton					
terbuthylazine					
ametryn	Fe_3O_4@MIL-100(Fe)	97.6−101.5	environmental water and vegetable samples	2.0−5.3 ppb	135, 2018
ATZ					
prometon					
simazine					
amidosulfuron	UiO-66-NH_2	75.7−94.2	spiked soil	0.19−1.79 ppb	136, 2017
metsulfuron methyl		82.2−95.3	water		
sulfosulfuron					
thifensulfuron methyl					
amidosulfuron	UiO-66-NH_2 magnetic stir bar	68.8−98.1	water and soil	0.04−0.84 ppb	137, 2018
metsulfuron methyl					
sulfosulfuron					
tribenuron methyl					
thifensulfuron methyl					
ATZ	magG@PDA@Zr-MOF	29−95	tobacco	10.78−45.45 $ng \cdot g^{-1}$	138, 2018
bifenthrin					
cyhalothrin					
parathion methyl					
penconazole					
pirimiphos					
procymidone					
trifluralin					
atraton	Fe_3O_4@SiO_2-GO/MIL-101(Cr)	83.9−103.5	rice	0.010−0.080 $\mu g\ kg^{-1}$	139, 2018
ATZ					
prometon					

https://doi.org/10.1021/acsami.2c00615
ACS Appl. Mater. Interfaces 2022, 14, 16983−17007

Table 3. continued

agrochemical	MOF/MOF composite	recovery (%)	applicability	detection limit	ref, year
secbumeton, terbuthylazine terbumeton trietazine					
ATZ prometryn	ZIF-8/SiO_2@Fe_3O_4	88.0−101.9	fruit, vegetables, and water	0.18−0.72 ppb	140, 2017
ATZ carbaryl chlorpyrifos 2,4-dichlorophenol 2,6-DN	$[Mg_2(APDA)_2(H_2O)_3]$		DMF solutions	150 ppb	141, 2018
ATZ bifenthrin bromuconazole clofentezine fenbuconazole flumetralin pirimicarb procymidone	$[(La_{0.9}Sm_{0.1})_2(DPA)_3(H_2O)_3]$	52.7−135.0	peppers (*Capsicum annuum L.*)	16.0−67.0 $\mu g \cdot kg^{-1}$	142, 2018
avermectin carbofuran clorpirifos fenvalerate pyridaben triadimefon	Zn-BTC	78.6−116.1 for industrial wastewater 87.5−107.9 for domestic sewage 97.5−101.1 for tap water	wastewater	0.20−1.60 ppb	143, 2017
azinphos methyl	$[Y_{1.8}Eu_{0.1}Tb_{0.1}(1,4\text{-}PDA)_3(H_2O)_1]$		aqueous media	212 ppb	144, 2019
azinphos-methyl	$[Cd_{2.5}(1,4\text{-}PDA)(tz)_3]$		aqueous media	16 ppb	145, 2017
azinphos-methyl chlorpyrifos parathion	$[Cd_3(1,4\text{-}PDA)_1(tz)_3Cl(H_2O)_4]$		apple and tomato	8 ppb	146, 2018
bensulfuron methyl chlorimuron ethyl nicosulfuron metsulfuron methyl pyrazosulfuron ethyl thifensulfuron methyl	MIL-53-PVDF MMM	77.20−111.00	tap, surface, and seawater	3.75−10.30 × 10^{-3} ppm	147, 2019
bensulfuron methyl chlorimuron ethyl pyrazosulfuron ethyl sulfometuron methyl	MIL-101(Fe)@PDA@Fe_3O_4	87.1−108.9	real water samples (lake, river, irrigation, and reservoir water) and vegetables (pak choi, spinach, and celery)	0.12−0.34 ppb	148, 2018
6-benzylaminopurin indole-3-acetic acid indolepropionic acid 3-indolebutyric acid	ZIF-8@SiO_2	70−120	oranges	3.0−59.4 ppb	149, 2018
bifenthrin fenvalerate isocarbophos parathion permethrin triazophos	UiO-66	60.9−117.5	vegetables	0.4−2.0 $ng \cdot g^{-1}$	150, 2021
bifenthrin deltamethrin fenpropathrin permethrin	MIL-101(Cr)-based composite	78.3−103.6	environmental water and tea samples	0.008−0.015 ppb	151, 2018
bifenthrin teflubenzuron thiacloprid	$[(Nd_{0.9}Eu_{0.1})_2(DPA)_3(H_2O)_3]$	78−88	soursop exotic fruit (*Annona muricata*)	0.03−0.05 $mg \cdot kg^{-1}$	152, 2015

https://doi.org/10.1021/acsami.2c00615
ACS Appl. Mater. Interfaces 2022, 14, 16983−17007

Table 3. continued

agrochemical	MOF/MOF composite	recovery (%)	applicability	detection limit	ref, year
thiamethoxam, thiophanate methyl					
bromopropylate clofentezine coumaphos difenoxuron diniconazole flumetralin fluometuron teflubenzuron	$[Zn(BDC)_x(NH_2\text{-}BDC)_{1-x}(H_2O)_2]n$	47−76	coconut palm	0.01−0.05 $\mu g \cdot g^{-1}$	153, 2017
butachlor metazachlor pretilachlor propanil	MIL-101(Zn)	86.9−119.0	black, red, and kidney beans	1.18 $\mu g \cdot kg^{-1}$ 0.58 $\mu g \cdot kg^{-1}$ 1.78 $\mu g \cdot kg^{-1}$ 0.90 $\mu g \cdot kg^{-1}$	154, 2019
butralin chlorothalonil chlorpyrifos deltamethrin pyridaben tebuconazole	Fe_3O_4@NH_2-MIL-101	70.5−119.8	aqueous solutions	0.13−0.86 ppb	155, 2020
carbendazim	MXene/CNHs/β-CD-MOFs	97.77−102.01	aqueous solution with coexisting substrates and tomato	1.0 nM	129, 2020
carbendazim	UiO-67	90.82−103.45	apple, cucumber, and cabbage	3.0×10^{-3} μM	156, 2021
carbaryl carbofuran	MIL-101(Fe)@GO	98.8−104.7	fruit and vegetables	1.2 and 0.5 nM	157, 2019
carbaryl matrine triadimefon	F1, F2, F3, and F4		aqueous solution	−, 108, 106, and 30 ppb	158, 2021
chloramphenicol	MIP/Zr-LMOF	95−105	milk and honey	13 ppb	159, 2021
chlorfluazuron flufenoxuron hexaflumuron lufenuron teflubenzuron triflumuron	ATP@Fe_3O_4@ZIF-8	78.8−114.3	tea infusions	0.7−3.2 ppb	127, 2020
chlorothalonil 2,6-DN nitrofen trifluralin	$(H_3O)[Zn_2L_1(H_2O)]$		aqueous solutions	2.93 ppm	160, 2019
chlorpyrifos	AChE@Basolite Z1200		tomato	3 $ng \cdot L^{-1}$	161, 2021
chlorpyrifos	Tb-MOF	82.17−93.6	tap water, cucumber, cabbage, kiwifruit, and apple	3.8 nM	162, 2019
chlorpyrifos	$[Ln(tftpa)_{1.5}(2,2'\text{-bpy})\ (H_2O)]$		ethanolic solutions, 5 cycles	0.14 ppb	163, 2018
chlorpyrifos	UiO-66-NH_2/Glycine/GO		aqueous solution	0.15 ppb	164, 2021
chlorpyrifos	CBZ-BOD@ZIF-8		aqueous solution	1.15 $ng \cdot mL^{-1}$	165, 2021
chlorpyrifos diazinon fenitrothion malathion	TMU-4/PES	88−108	water and soil samples	5−8 ppb	166, 2018
chlorpyrifos phosalone	Cu/$CuFe_2O_4$@MIL-88A(Fe)	88.3−100.4	water samples (farm water, water of rice field, and river water) and fruit juice and vegetable samples (pomegranate, kiwi, orange, tomato, and cucumber)	0.2 and 0.5 ng mL^{-1}	167, 2021
chlorfluazuron clofentezine diflubenzuron forchlorfenuron hexaflumuron lufenuron	Fe_3O_4@MOF-808	84.6−98.3	tea beverages and juice samples	0.04−0.15 ppb	168, 2020

https://doi.org/10.1021/acsami.2c00615
ACS Appl. Mater. Interfaces 2022, 14, 16983−17007

Table 3. continued

agrochemical	MOF/MOF composite	recovery (%)	applicability	detection limit	ref, year
penfluoron					
clethodim	MIL-125(Ti)-NH_2@TiO_2	96.8−103.5	aqueous solutions	10 nM	169, 2015
cyhalothrin	MOFs-MIPs-MSPD	>93	wheat	1.8−2.8 ng g^{-1}	170, 2019
β-cyfluthrin					
cyphenothrin					
2,4-D	MOF-808	77.1−109.3	mixed juice, orange juice, and tap water	0.1−0.5 ppb	171, 2019
2-DPP					
4-CPA					
dicamba					
2,4-D	UiO-66@cotton	83.3−106.8	cucumber and tap water	0.1−0.3 ppb	172, 2020
2-DPP					
4-CPA					
dicamba					
2,4-D	UiO-67	86.12−103.44	tomato, cucumber, and white gourd	0.1−0.5 ppb	173, 2018
2-DPP					
4-CPA					
dicamba					
2,4-D	UiO-66-NH_2	82.3−102	tomato, Chinese cabbage, and rape	0.16−0.37 ng·g^{-1}	174, 2017
MCPA					
MCPB					
MCPP					
p,p′-DDD	M-M-ZIF-67	75.1−112.7	tap, river, and agricultural irrigation water samples	0.07−1.03 ppb	175, 2018
o,p′- and *p,p′*-DDE					
o,p′- and *p,p′*-DDT					
α-, β-, γ-, and δ-HCH					
diazininon	UiO-66	85.7−97.8	tap and river water and tomato, apple, and tomato juice	2.5 ng·mL^{-1}	176, 2021
diazinon	MIL-101@GO-HF-SPME	88−104	tomato, cucumber, and agricultural water	0.21 ppm	177, 2020
chlorpyrifos				0.27 ppm	
diazinon	ZIF-8	91.9−99.5	tap, waste, and river waters and apple, peach, and grape juices	0.03−0.21 ppb	178, 2019
fenthion	Zn-based MOFs				
fenitrothion					
profenofos					
phosalone					
diniconazole	Fe_3O_4-MWCNT@MOF-199	62.80−94.20	eabbage, spinach, and orange and apple juices	520−1830 ppb	179, 2021
fenbuconazole					
flusilazole					
hexaconazole					
penconazole					
propiconazole					
tebuconazole					
2,6-DN	$[Zn_2(L)_2(TPA)]$		recyclable (5 cycles), detection in methanol or chloroform solutions	0.39 ppm	180, 2019
2,6-DN	$[Zn_2(bpdc)_2(BPyTPE)]$		dichloromethane	0.13−0.8 ppm	124, 2017
2,6-DN	$[Cd(tptc)_{0.5}(bpz)(H_2O)]$		aqueous media	638 ppb	181, 2020
2,6-DN	Cd-CBCD		aqueous media; recyclability (5 cycles)	145 ppb	182, 2019
2,6-DN	$[Ag(CIP^-)]$		DMF	1.7×10^{-7} M	183, 2019
2,6-DN	$[Ln_3(HDDB)(DDB)(H_2O)_6]$ (Ln = Eu, Tb, Dy, Gd)	98−103.1	aqueous solution, nectarines, carrots, and grapes	86 ppb	184, 2021
2,6-DN	$[Eu_2(dtztp)(OH)_2(DMF)(H_2O)_{2.5}]$		lake water, 5 cycles	5.28 ppm	185, 2021
dichlorvos	Fe_3O_4/MIL-101	76.8−94.5	hair	0.21−2.28 ppb	126, 2014
methamidophos		74.9−92.1	urine		
dimethoate					
malathion					
parathion					
parathion methyl					

https://doi.org/10.1021/acsami.2c00615
ACS Appl. Mater. Interfaces 2022, 14, 16983−17007

Table 3. continued

agrochemical	MOF/MOF composite	recovery (%)	applicability	detection limit	ref, year
difenoconazole	M-IRMOF	74.82−99.52	vegetable	0.25 ppb	186, 2019
epoxiconazole				0.25 ppb	
fenbuconazole				1.0 ppb	
pyraclostrobin				0.25 ppb	
thiabendazole				0.25 ppb	
diniconazole	UiO-66@polymer	90.4−97.5	water	1.34−14.8 × 10^{-3} ppm	187, 2019
flutriafol		84.0−95.3	soil		
hexaconazole					
pyrimethanil					
tebuconazole					
diniconazole	MOF-5@GO	85.6−105.8	grape, apple, cucumber, celery, cabbage, and tomato	0.05−1.58 ng·g^{-1}	188, 2016
hexaconazole					
myclobutanil					
propiconazole					
triadimefon					
diniconazole	defective UiO-66	82.6−92.2, 82.8−98.2, and 80.2−88.2 for pond, river, and lotus pond waters	environmental water samples	4−36 ppb	189, 2021
pyrimethanil					
tebuconazole					
dinotefuran	$[(CH_3)_2NH_2]_2[Cd_3(BCP)_2]$		water	2.09 ppm	190, 2021
α- and β-endosulfan	$[(La_{0.9}Eu_{0.1})_2(DPA)_3(H_2O)_3]$	70−107	lettuce	0.02 mg·kg^{-1}	123, 2010
malathion					
parathion methyl					
procymidone					
pyrimicarb					
epoxiconazole	Fe_3O_4@APTES-GO/ZIF-8	71.2−110.9	tap water, honey samples, and mango, grape, and orange juices; recyclability (5 cycles)	0.014−0.109 ppb	128, 2020
flusilazole					
tebuconazole					
triadimefon					
fenitrothion	$[Cd(BDC\text{-}NH_2)(H_2O)_2]_n$		ethanolic solutions	1 ppb	191, 2014
parathion methyl					
paraoxon					
parathion					
fenitrothion	MOF-5		aqueous solutions	5 ppb	192, 2014
parathion methyl					
paraoxon					
parathion					
fenitrothion	SPP@Au@MOF-5	97.5	soil	10^{-12} M	193, 2019
paraoxon ethyl					
GLY	MOF-Calix		aqueous solutions	0.38 ppm	194, 2020
GLY	$[Tb(L)_2NO_3]_n$ (HL)		aqueous solutions	0.0144 μM	195, 2021
glufosinate	MOF-545		aqueous solutions	0.0009 ppb	196, 2021
GLY					
imidacloprid	UiO-66-NH_2	92.39	fruit samples	40−60 ppb	197, 2021
thiamethoxam		94.37			
iprodione	MIL-101-NH_2@Fe_3O_4-COOH	71.1−99.1	real water samples	0.04−0.4 ppb	198, 2018
myclobutanil					
prochloraz					
tebuconazole					
malathion	BTCA-P-Cu-CP	91.0−104.4	vegetable extracts (spinach, celery, lettuce, red capsicum, eggplant, and cherry tomato)	0.17−0.59 nM	199, 2019
malathion	Basolite C300	>92%	water, fruits, and vegetables	4.0 ppb	200, 2020
malathion	Pt@UiO-66-NH_2	93.34−97.80	aqueous solutions	4.9 × 10^{-15} M	201, 2019
MCPA	HKUST-1	57−100	water, soil, rice, and tomato	10 × 10^{-3} ppm	202, 2018
monocrotophos,	MIL-101(Cr)@MIP	86.5−91.7	apple and pear	0.011 mg·kg^{-1}	203, 2017
trichlorfon				0.015 mg·kg^{-1}	
molinate	ZIF-67@$MgAl_2O_4$		aqueous solutions	3 ppm	204, 2021

https://doi.org/10.1021/acsami.2c00615
ACS Appl. Mater. Interfaces 2022, 14, 16983−17007

Table 3. continued

agrochemical	MOF/MOF composite	recovery (%)	applicability	detection limit	ref, year
nicosulfuron	Tb-BDOA		aqueous solutions	1.61	205, 2021
thiamethoxam				1.04 μM	
nitrofen	PVP/Glu/CRL@ZIF-8	92.15−107.58	aqueous solutions	0,14 μM	206, 2021
p-nitrophenyl phosphate	[Co(OBA)(2,2′-BPY)]	93.6−131.6	fruits (watermelon, orange, tomato, and apple)	352 nM (0.07 mg kg^{-1})	207, 2021
bis(*p*-nitrophenyl) phosphate			real water samples		
parathion methyl	$[Cd(2,2',4,4'\text{-bptcH}_2)]_n$		aqueous solutions	0.006 ppb	122, 2010
parathion methyl	ZnPO-MOFs	93.0−104.6	irrigation water	0.12 μg kg^{-1} (0.456 nM)	208, 2018
parathion methyl	Au/Cys-Fe_3O_4/MIL-101		juice samples	5 ppb	209, 2021
parathion methyl	Zr-BDC-rGO	95.3−103.4	aqueous solutions	0.5 ng mL^{-1}	210, 2021
parathion methyl	$Ru(bpy)_3^{2+}$-ZIF-90	93.3−103.6	aqueous solutions	0.037 ng mL^{-1}	211, 2021
paraquat	$[Zn_2(cptpy)(BTC)(H_2O)]_n$		aqueous solutions	9.73×10^{-6} M	212, 2019
parathion methyl	Zr-LMOF	78−107	cowpea and lettuce	0.115 μg·kg^{-1}	125, 2019
parathion					
parathion	$[Cd(BDC\text{-}NH_2)(H_2O)_2]_n$		rice	0.1 ppb	213, 2015
quinalphos	CD@UiO-66-NH_2	98−105	tomato and rice	0.3 nM	214, 2021
NIT	PCN-224	97.76−104.02	paddy water	0.03×10^{-3} ppb	62, 2020
		88.1−100.30	soil		
NIT	Rho B@1	95.2−102.0	river water	0.27 μg·kg^{-1}	215, 2020
	Rho 6G@1	93.4−103.5		0.86 μg·kg^{-1}	
thiabendazole	Tb^{3+}@UiO-66-$(COOH)_2$	98.41−104.48	orange and aqueous solutions	0.271 μM	216, 2021
thiabendazole	Ag-Au-IP6-MIL-101(Fe)	84.4−112.8	juice	50 ppb	217, 2019

[a]The table is organized according to the agrochemical studied, followed by the MOF-based material name (or chemical formula), recovery (%), applicability, and detection limit. 2,2′-BPY: 2,2′-bipyridyl; $2,2',4,4'\text{-bptcH}_2$: 2,2′,4,4′-biphenyltetracarboxylic acid; AChE: acetylcholinesterase; APTES: (3-aminopropyl)triethoxysilane; ATP: attapulgite; BPyTPE: (*E*)-1,2-diphenyl-1,2-bis(4-(pyridin-4-yl)phenyl)ethene; bpz: 2-(1*H*-pyrazol-3-yl)pyridine; CD: carbon dots; CNHs: carbon nanohorns; CP: coordination polymer; CRL: *Candida rugosa lipase*; DMF: *N*,*N*′-dimethylformamide; GO: graphene oxide; H_2BDC: bezene-1,4-dicarboxylic acid; $H_2BDC\text{-}NH_2$: 2-aminoterephthalic acid; H_2bpdc: biphenyl-4,4′-dicarboxylic acid; H_2DPA: pyridine-2,6-dicarboxylic acid; H_3BTC: 1,3,5-benzenetricarboxylic acid; H_4BTCA: benzene-1,2,4,5 tetracarboxylic acid; HCIP: 4-(4-carboxylphenyl)-2,6-di(4-imidazol-1-yl)phenyl pyridine; H_3CBCD: 4,4′-(9-(4′-carboxy-[1,1′-biphenyl]-4-yl)-9*H*-carbazole-3,6-diyl)dibenzoic acid; H_4dtztp: 2,5-bis(2*H*-tetrazol-5-yl) terephthalic acid; Hcptpy: 4-(4-carboxyphenyl)-2,2′:4′,4″-terpyridine; H_5DDB: 3,5-di(2′,4′-dicarboxylphenyl) benzoic acid; HL: 3.5-bis(triazol-1-yl) benzoic acid; H_2tftpa: tetrafluoroterephthalic acid; H_4tptc: *p*-terphenyl-2,2′,5″,5‴-tetracarboxylate acid; H_2APDA: 4,4′-(4-aminopyridine-3,5-diyl)dibenzoic acid; H_4BCP: 5-(2,6-bis(4-carboxyphenyl)pyridin-4-yl)-isophthalic acid; HF: hollow fiber; IP_6: inositol hexaphosphate; L_1H_5: 2,5-(6-(4-carboxyphenylamino)-1,3,5-triazine-2,4-diyldiimino)diterephthalic acid; L: 4-(tetrazol-5-yl)phenyl-4,2′:6′,4″-terpyridine; polymer: poly(*N*-vinylcarbazole-*co*-divinylbenzene); magG: magnetic graphene; MIP: molecularly imprinted polymer; MMM: mixed-matrix membranes; MSPD: matrix solid-phase dispersion; OBA: 4,4′-oxybis(benzoic acid); PBS: phosphate buffer saline; PDA: polydopamine; 1,4-PDA: 1,4-phenylenediacetate; PES: poly(ether sulfone); PVDF: poly(vinylidene fluoride); Rho: rhodamine; SPME: solid-phase microextraction; SPP: surface plasmon polariton; TPA: terephthalic acid; tz: 1,2,4-triazolate.

detection of OP pesticides.[125] Along the 22 pesticides tested, the synthesized CAU-24 quickly absorbs trace amounts of OP parathion methyl and indicates its presence. It has a low LOD of 0.115 μg·kg^{-1} (0.438 nM) with a wide linear range from 70 μg·kg^{-1} to 5.0 mg·kg^{-1}. The water stability of this Zr-MOF was investigated by suspending it in water for 24 h and monitoring by powder X-ray diffraction (PXRD), adsorption/desorption isotherms, and pore distribution. The crystalline structure and porosity of the Zr-MOF was kept in water after 24 h. Finally, the Zr-MOF was used to mimic rapid *in situ* imaging detection of pesticide residues on surface vegetables (lettuce and cowpea); visual signals appeared under UV light within 5 min. Therefore, this MOF has the possibility for low-cost, rapid, and *in situ* imaging detection of OP contamination via easy-to-read visual signals.

MOF composites have also been used in the determination of agrochemicals. In 2014, a MOF with an iron oxide enclosure was reported for the determination of OPs in biological samples.[126] In this work, MIL-101(Fe) was modified as a model with superparamagnetic qualities using Fe_3O_4 to form a homogeneous magnetic product (Fe_3O_4/MIL-101 composite). The Fe_3O_4/MIL-101 composite was investigated for the magnetic solid-phase extraction of six OPs from human hair and urine samples followed by gas chromatography analysis. Under optimized conditions (desorption solvent, extraction time, desorption time, etc.), this method showed low LOD (0.21−228 ng·mL^{-1}), wide linearity, and good precision (1.8−8.7% for intraday, 2.9−9.4% for interday). The adequate recoveries of the spiked samples were 76.8−94.5% and 74.9−92.1% for hair and urine, respectively, suggesting that the

https://doi.org/10.1021/acsami.2c00615
ACS Appl. Mater. Interfaces 2022, 14, 16983−17007

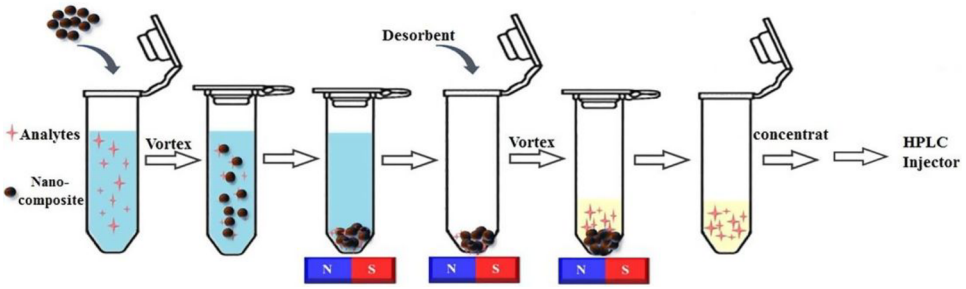

Figure 8. Schematic view of the MSPE procedure when using ATP@Fe_3O4@@ZIF-8 in benzoylureas determination (N: North; S: South). Reprinted with permission from ref 127. Copyright 2020 Elsevier Ltd.

Fe_3O_4/MIL-101 sorbent is feasible for the analysis of trace OPs in biological samples. Other Fe_3O_4-MOF-based composites have recently been reported for the efficient determination of different agrochemicals, for example, the magnetic solid-phase extraction method based on the attapulgite-modified MOF (ATP@Fe_3O_4@ZIF-8) in the determination of bezoylureas (insecticides; see Table 3).[127] ATP, an eco-friendly nature and low-cost clay, is added here to improve the hydrolytic stability of ZIF-8 as the −OH groups of ATP can selectively coordinate with the metal ions in ZIF-8. The ATP@Fe_3O_4@ZIF-8 nanocomposite was applied as a sorbent for the magnetic solid-phase extraction (MSPE) of benzoylureas prior to high-performance liquid chromatography (HPLC) determination (Figure 8). The established method was validated in terms of linearity (2.5−500 $\mu g\ L^{-1}$ with satisfactory recovery of 88.29−95.99%) and precision (relative standard deviation, RSD, of <8%). Moreover, after 5 cycles, there was hardly any noticeable loss of the extraction efficiency. Finally, this method was effectively used in the determination of 6 benzoylureas in different tea infusions; the determined relative recoveries ranged from 78.8% to 114.3%.

Another example of magnetic solid-phase extraction using Fe_3O_4@ZIF-8-based composites is the work reported by Senosy et al. on the basis of the synthesis of Fe_3O_4@APTES-GO/ZIF-8 (APTES: (3-aminopropyl)triethoxysilane; GO: graphene oxide) and its evaluation as an adsorbent for the determination of triazole fungicides in water, honey, and fruit juices.[128] Here, GO sheets were used to improve the dispersion of the adsorbent in aqueous solutions and, again, ZIF-8 to ensure enough surface area and active sites. Under the optimum conditions (extraction time, pH value of the sample, etc.), the obtained linearity of this method ranged from 1 to 1000 $\mu g{\cdot}L^{-1}$ for all analytes. The LODs and LOQs of four triazole fungicides ranged from 0.014 to 0.109 $\mu g\ L^{-1}$ and from 0.047 to 0.365 $\mu g\ L^{-1}$, respectively. Moreover, this adsorbent could be reused without significant loss of its extraction recoveries. When compared with the outcomes from other studies, Fe_3O_4@APTES-GO/ZIF-8-MSPE could provide a higher performance and achieve satisfactory results for the analysis of trace triazole fungicides in complex matrices. Another composite, based on a nanoarchitecture of Mxene/carbon nanohorns/β-cyclodextrin-MOF (MXene/CNHs/β-CD-MOFs), was utilized as an electrochemical sensing platform for the determination of carbendazim pesticide.[129] β-CD-MOFs combined the properties of the host−guest recognition of β-CD and porous structure, high porosity, and pore volume of MOFs, which are fundamental in achieving a high adsorption capacity of carbendazim. MXene/CNHs possess a large specific surface area, accessible active sites, and high conductivity, which allowed more mass transport channels and enhanced the mass transfer capacity and catalysis of carbendazim.[123,126,128] With the collaborative effect of both (β-CD-MOFs and MXene/CNHs), the electrode extended a wide linear range from 3.0 nM to 10.0 μM and a low LOD of 1.0 nM. Additionally, this sensor also showed high selectivity, reproducibility, and long-term stability as well as satisfactory application in tomato samples.

7. PERSPECTIVES IN USING MOFs IN AGRICULTURE

As a novel class of materials, MOFs exhibit a great potential in agroindustry, either to detect or eliminate agrochemicals or to achieve their sustained and controlled release. In all these scenarios, the aim is to reach the rational and environmentally friendly use of agrochemicals. Despite the novelty of MOFs in agriculture, the experience acquired in other areas (particularly biomedical and environmental ones) allow us to identify precise challenges related to their use in agriculture.

First, MOF stability under the working conditions is of crucial relevance. However, from the wide number of MOFs and MOF-based composites reported in environmental remediation (water and soil), only few discuss this critical point and mostly under conditions far from real water streams or fields. In this sense, many of these materials are built up from toxic metals (e.g., Cr, Ag) and/or harmful organic moieties (e.g., porphyrins), which can be released upon the MOF degradation. The selection of safe and stable MOFs is therefore mandatory for their use in agroindustry (mainly for environmental remediation and agrochemical controlled release). Further, it is essential to investigate the performance of MOFs under real conditions using complex water and soil compositions and/or vegetables or plants (e.g., river water, real fields or greenhouses, vegetables, products, etc.), considering concentration ranges found in nature, different temperatures, humidity, sunlight hours, soil composition, or pH in different parts of plants, among others.

Second, the cost of MOFs is of particular importance for agroindustry applications. When one takes into account that vegetables and fruits are normally popular and affordable, it is necessary to use a low-cost and long-lifetime material. Nontoxic and abundant safe precursors together with simple synthetic routes with a high space time yield (STY; kilogram of MOF produced per cubic meter of reaction per day) (toxic solvents, expensive ligands, etc.) need to be put in place for the most promising candidates. Note here that few MOFs have been produced so far at the ton scale by different companies, and thus, they are not currently commercially available.[218] To further progress through the application, specific manufacturing and devices should be considered (pellets, columns,

https://doi.org/10.1021/acsami.2c00615
ACS Appl. Mater. Interfaces 2022, 14, 16983−17007

membranes, etc.), and one needs to take into account the potential decrease in the MOF performance.

Finally, understanding the interaction of the agrochemicals and MOFs might help one further improve the resulting performances at the detection, removal, or progressive release stages. Also, research could be focused on multifunctional MOFs and MOF composites that combine, for instance, the extraction with the detection of pesticides in food matrices or the simultaneous elimination of different agrochemicals.

Although there are challenges to the use of MOFs in agriculture, this new domain in the application of MOFs will continue, and it is expected that novel knowledge and development will soon be the outcome. This Review opens fascinating perspectives for the safe and efficient MOF application in agriculture.

AUTHOR INFORMATION

Corresponding Authors

Sara Rojas − *Biochemistry and Electronics as Sensing Technologies Group, Department of Inorganic Chemistry, University of Granada, 18071 Granada, Spain;* orcid.org/0000-0002-7874-2122; Email: srojas@ugr.es

Patricia Horcajada − *Advanced Porous Materials Unit (APMU), IMDEA Energy, 28935 Móstoles, Madrid, Spain;* orcid.org/0000-0002-6544-5911; Email: patricia.horcajada@imdea.org

Author

Antonio Rodríguez-Diéguez − *Biochemistry and Electronics as Sensing Technologies Group, Department of Inorganic Chemistry, University of Granada, 18071 Granada, Spain;* orcid.org/0000-0003-3198-5378

Complete contact information is available at: https://pubs.acs.org/10.1021/acsami.2c00615

Notes

The authors declare no competing financial interest.

ACKNOWLEDGMENTS

The work has been supported by the MOFSEIDON project (PID2019-104228RB-100) funded by MCI/AEI/10.13039/501100011033/FEDER "Una manera de hacer Europa", ESENCE project (RTC2019-007254-5) funded by MCIN/AEI/10.13039/501100011033), Junta de Andalucía (FQM-394), and the Multifunctional Metallodrugs in Diagnosis and Therapy Network (MICIU, RED2018-102471-T). P.H. acknowledges the Spanish Ramón y Cajal Programme (grant agreement 2014-15039). S.R. acknowledges the Spanish Juan de la Cierva Incorporación Fellowship (grant agreement no. IJC2019-038894-I) funded by MCIN/AEI/10.13039/501100011033. Funding for open access charge: Universidad de Granada/CBUA.

ABBREVIATIONS

2,2′-BPY, 2,2′-bipyridyl; 1,3-DCPP, *cis*-1,3-dichloropropene; 1,4-PDA, 1,4-phenylenediacetate; 2-DPP, desmetryn,2-(2,4-dichlorophenoxy)propionic acid; 2,2′,4,4′-bptcH_4, 2,2′,4,4′-biphenyltetracarboxylic acid; 2,4-D, 2,4-dichlorophenoxyacetic acid; 2,6-DN, 2,6-dichloro-4-nitroaniline; 4-CPA, 4-chlorophenoxyacetic acid; β-CD, β-cyclodextrin; AChE, acetylcholinesterase; AMPA, aminomethylphosphonic acid; APTES, (3-aminopropyl)triethoxysilane; ATP, attapulgite; ATZ, atrazine; Bp, black phosphorus; Bpd, 1,4-bis(4-pyridyl)-2,3-diaza-1,3-butadiene; BPyTPE, (*E*)-1,2-diphenyl-1,2-bis(4-(pyridin-4-yl)-phenyl)ethene; bpz, 2-(1*H*-pyrazol-3-yl)pyridine; BSA, bovine serum albumin; C, chitosan; CA, cellulose acetate; CDs, carbon dots; CMCS, carboxymethyl chitosan; CNHs, carbon nanohorns; CP, coordination polymer; CPO, chloroperoxidase enzyme; CRL, *Candida rugosa lipase*; DDE, dichloro-2,2-bis(*p*-chlorophenyl)ethylene; DDT, 1,1,1-trichloro-2,2-bis(*p*-chlorophenyl)ethylene; DMF, *N*,*N*′-dimethylformamide; DUR, diuron; ED_{50}, concentration for 50% of maximal effect; EDTA, ethylenediaminetetraacetate; EU, European Union; FAO, Food and Agriculture Organization; Fe-SPC, Fe-doped nanospongy porous biocarbon; GC/MS, gas chromatography−mass spectrometry; GLU, glufosinate; GLY, glyphosate; GO, graphene oxide; GSH, glutathione; H_2APDA, 4,4′-(4-aminopyridine-3,5-diyl)dibenzoic acid; H_2BDC, benzene-1,4-dicarboxylic acid; H_2BDC-NH_2, 2-aminoterephthalic acid; H_2DPA, pyridine-2,6-dicarboxylic acid; H_2bpdc, biphenyl-4,40-dicarboxylic acid; H_2DPA, pyridine-2,6-dicarboxylic acid; H_2TCPP, tetrakis(4-carboxyphenyl)porphyric; H_2tftpa, tetrafluoroterephthalic acid; H_3BTC, 1,3,5-benzenetricarboxylic acid; H_3CBCD, 4,4′-(9-(4′-carboxy-[1,1′-biphenyl]-4-yl)-9*H*-carbazole-3,6-diyl)dibenzoic acid; H_4BCP, 5-(2,6-bis(4-carboxyphenyl)pyridin-4-yl)-isophthalic acid; H_4BTCA, benzene-1,2,4,5 tetracarboxylic acid; H_4dtztp, 2,5-bis(2*H*-tetrazol-5-yl) terephthalic acid; H_4TCPB, 1,2,4,5-tetrakis(4-carboxyphenyl)benzene; H_4tptc, *p*-terphenyl-2,2″,5″,5‴-tetracarboxylate acid; H_5DDB, 3,5-di(2′,4′-dicarboxylphenyl) benzoic acid; HCH, hexachlorocyclohexane; HCIP, 4-(4-carboxylphenyl)-2,6-di(4-imidazol-1-yl)phenyl pyridine; Hcptpy, 4-(4-carboxyphenyl)-2,2′:4′,4″-terpyridine; HF, hollow fiber; HKUST, Hong Kong University of Science and Technology; HL, 3.5-bis(triazol-1-yl) benzoic acid; HLF-1, human lung fibroblast; Hmim, 2-methylimidazole; HPLC, high-performance liquid chromatography; HRP, horseradish peroxidase enzyme; IC_{50}, half maximal inhibitory concentration; ILCS, ionic liquid modified chitosan; Im, imidazonate; IP_6, inositol hexaphosphate; IPU, isoproturon; KT_{50}, knockdown time 50%; L_1H_5, 2,5-(6-(4-carboxyphenylamino)-1,3,5-triazine-2,4-diyldiimino)diterephthalic acid; L, 4-(tetrazol-5-yl)phenyl-4,2′:6′,4″-terpyridine; LC_{50}, median lethal concentration; LOD, limit of detection; LOQ, limit of quantification; magG, magnetic graphene; MCPA, 2-methyl-4-chlorophenoxyacetic acid; MCPB, (2-methyl-4-chlorophenoxy) butyric acid; MCPP, (2-methyl-4-chlorophenoxy) propionic acid; MIP, molecularly imprinted polymer; M-M, magnetic multiwalled carbon nanotubes; MMM, mixed-matrix membranes; MOFs, metal−organic frameworks; MSPD, matrix solid-phase dispersion; MSPE, magnetic solid-phase extraction; NIR, near-infrared; NIT, nitenpyram; NND, neonicotinoids; NPs, nanoparticles; OBA, 4,4′-oxybis(benzoic acid); OPs, organophosphorus pesticides; OPA, oxalate-phosphate-amine; P, pectin; PAN, polyacrylonitrine; PBS, phosphate buffer saline; PD, prochloraz (P) and 2,4-dinitrobenzaldehyde (D); PDA, polydopamine; PES, poly(ether sulfone); polymer, poly(*N*-vinylcarbazole-*co*-divinylbenzene); *p*,*p*′-DDD, *p*,*p*′-1,1-dichloro-2,2-bis(*p*-chlorophenyl)ethylene; PS, photosensitizer; PVDF, poly(vinylidene fluoride); XRD, powder X-ray diffraction; PyTBA, 4,4′,4′,4′-(pyrene-1,3,6,8-tetrayl)-tetrabenzoate; QPE, quizalofop-P-ethyl; QpeH, quizolafop-P-ethyl hydrolase esterase; Rho, rhodamine; RSD, relative standard deviation; RT, room temperature; S_{BET}, Brunauer−Emmett−Teller surface area; SL, sodium lignosulfonate; SPE,

https://doi.org/10.1021/acsami.2c00615
ACS Appl. Mater. Interfaces 2022, 14, 16983−17007

solid-phase extraction; SPME, solid-phase microextraction; SPP, surface plasmon polariton; STY, space time yield; TA, tannic acid; TCPB, 1,2,4,5-tetrakis(4-carboxyphenyl)benzene; Tebuc, tebuconazole; THI, thifluzamide; TMPyP, 5,10,15,20-tetrakis(1-methyl-4-pyridinio)porphyrin tetra(*p*-toluenesulfonate); TPA, terephthalic acid; tz, 1,2,4-triazolate; us, ultrasound; V_p, pore volume; ZIFs, zeolitic imidazolate frameworks

REFERENCES

(1) Caliman, F. A.; Robu, B. M.; Smaranda, C.; Pavel, V. L.; Gavrilescu, M. Soil and Groundwater Cleanup: Benefits and Limits of Emerging Technologies. *Clean Technol. Environ. Policy* **2011**, *13* (2), 241−268.

(2) Srivastav, A. L. Chemical Fertilizers and Pesticides: Role in Groundwater Contamination. In *Agrochemicals Detection, Treatment and Remediation*; Elsevier, 2020; DOI: 10.1016/b978-0-08-103017-2.00006-4.

(3) Carson, R. *Silent Spring*; Fawcett Crest, 1962;.

(4) van Emden, H. F.; Peakall, D. B. *Beyond Silent Spring: Integrated Pest Management and Chemical Safety*; Chapman & Hall, 1996; DOI: 10.1007/978-94-009-0079-0.

(5) Foley, J. A.; Ramankutty, N.; Brauman, K. A.; Cassidy, E. S.; Gerber, J. S.; Johnston, M.; Mueller, N. D.; O'Connell, C.; Ray, D. K.; West, P. C.; Balzer, C.; Bennett, E. M.; Carpenter, S. R.; Hill, J.; Monfreda, C.; Polasky, S.; Rockström, J.; Sheehan, J.; Siebert, S.; Tilman, D.; Zaks, D. P. M. Solutions for a Cultivated Planet. *Nature* **2011**, *478* (7369), 337−342.

(6) Servin, A.; Elmer, W.; Mukherjee, A.; De la Torre-Roche, R.; Hamdi, H.; White, J. C.; Bindraban, P.; Dimkpa, C. A Review of the Use of Engineered Nanomaterials to Suppress Plant Disease and Enhance Crop Yield. *J. Nanoparticle Res.* **2015**, *17* (2), 1−21.

(7) European Environmental Agency. *Pesticides Sales*; 2018; https://www.eea.europa.eu/airs/2018/environment-and-health/pesticides-sales.

(8) Younes, M.; Galal-Gorchev, H. Pesticides in Drinking Water - A Case Study. *Food Chem. Toxicol.* **2000**, *38* (Suppl.1), S87−S90.

(9) Aktar, W.; Sengupta, D.; Chowdhury, A. Impact of Pesticides Use in Agriculture: Their Benefits and Hazards. *Interdiscip. Toxicol.* **2009**, *2* (1), 1−12.

(10) Pimentel, D. Environmental and Economic Costs of the Application of Pesticides Primarily in the United States. *Environ. Dev. Sustain.* **2005**, *7* (2), 229−252.

(11) United Nations Human Right Council. *Report of the Special Rapporteur on the Right to Food (A/HRC/34/48)*; 2017; https://reliefweb.int/report/world/report-special-rapporteur-right-food-ahrc3448.

(12) Kapsi, M.; Tsoutsi, C.; Paschalidou, A.; Albanis, T. Environmental Monitoring and Risk Assessment of Pesticide Residues in Surface Waters of the Louros River (N.W. Greece). *Sci. Total Environ.* **2019**, *650*, 2188−2198.

(13) Poiger, T.; Buerge, I. J.; Bächli, A.; Müller, M. D.; Balmer, M. E. Occurrence of the Herbicide Glyphosate and Its Metabolite AMPA in Surface Waters in Switzerland Determined with On-Line Solid Phase Extraction LC-MS/MS. *Environ. Sci. Pollut. Res.* **2017**, *24* (2), 1588−1596.

(14) Comoretto, L.; Chiron, S. Comparing Pharmaceutical and Pesticide Loads into a Small Mediterranean River. *Sci. Total Environ.* **2005**, *349* (1−3), 201−210.

(15) Comoretto, L.; Arfib, B.; Chiron, S. Pesticides in the Rhône River Delta (France): Basic Data for a Field-Based Exposure Assessment. *Sci. Total Environ.* **2007**, *380* (1−3), 124−132.

(16) Food and Agricultural Organization of the United Nations. *Evaluation of FAO's Asia Regional Integrated Pest Management and Pesticide Risk Reduction Programme in the Greater Mekong Subregion*; FAO, 2020; DOI: 10.4060/ca7783en.

(17) Kumar, V.; Kumar, P. Pesticides in Agriculture and Environment: Impacts on Human Health. In *Contaminants in Agriculture and Environment: Health Risks and Remediation*; Agro Environ Media, 2019; pp 76−95; DOI: 10.26832/aesa-2019-cae-0160-07.

(18) García, A. M. Pesticide Exposure and Women's Health. *Am. J. Ind. Med.* **2003**, *44* (6), 584−594.

(19) Figueroa, Z. I.; Young, H. A.; Mumford, S. L.; Meeker, J. D.; Barr, D. B.; Gray, G. M.; Perry, M. J. Pesticide Interactions and Risks of Sperm Chromosomal Abnormalities. *Int. J. Hyg. Environ. Health* **2019**, *222* (7), 1021−1029.

(20) Bassil, K. L.; Vakil, C.; Sanborn, M.; Cole, D. C.; Kaur, J. S.; Kerr, K. J. Cancer Health Effects of Pesticides: Systematic Review. *Can. Fam. Physician* **2007**, *53* (10), 1705−1711.

(21) De Roos, A. J.; Zahm, S. H.; Cantor, K. P.; Weisenburger, D. D.; Holmes, F. F.; Burmeister, L. F.; Blair, A. Integrative Assessment of Multiple Pesticides as Risk Factors for Non-Hodgkin's Lymphoma among Men. *Occup. Environ. Med.* **2003**, *60* (9), 1−9.

(22) Tilman, D.; Cassman, K. G.; Matson, P. A.; Naylor, R.; Polasky, S. Agricultural Sustainability and Intensive Production Practices. *Nature* **2002**, *418*, 671−677.

(23) European Commission. *Fertilisers in the EU: Prices, Trade and Use*; EC, 2019; https://ec.europa.eu/info/sites/default/files/food-farming-fisheries/farming/documents/market-brief-fertilisers_june2019_en.pdf.

(24) Derosa, M. C.; Monreal, C.; Schnitzer, M.; Walsh, R.; Sultan, Y. Nanotechnology in Fertilizers. *Nat. Nanotechnol.* **2010**, *5* (2), 91.

(25) Monreal, C.; McGill, W. B.; Nyborg, M. Spatial Heterogeneity of Substrates: Effects on Hydrolysis, Immobilization and Nitrification of Urea-N. *Can. J. Soil. Sci.* **1986**, *66*, 499−511.

(26) Food and Agricultural Organization of the United Nations. *World Agriculture: Towards 2015/2030 Summary Report*; FAO, 2002; https://www.fao.org/3/y3557e/y3557e00.pdf.

(27) Machell, J.; Prior, K.; Allan, R.; Andresen, J. M. The Water Energy Food Nexus-Challenges and Emerging Solutions. *Environ. Sci. Water Res. Technol.* **2015**, *1* (1), 15−16.

(28) Yin, J.; Wang, Y.; Gilbertson, L. M. Opportunities to Advance Sustainable Design of Nano-Enabled Agriculture Identified through a Literature Review. *Environ. Sci. Nano* **2018**, *5* (1), 11−26.

(29) Rodrigues, S. M.; Demokritou, P.; Dokoozlian, N.; Hendren, C. O.; Karn, B.; Mauter, M. S.; Sadik, O. A.; Safarpour, M.; Unrine, J. M.; Viers, J.; Welle, P.; White, J. C.; Wiesner, M. R.; Lowry, G. V. Nanotechnology for Sustainable Food Production: Promising Opportunities and Scientific Challenges. *Environ. Sci. Nano* **2017**, *4* (4), 767−781.

(30) Li, Z.-Z.; Chen, J.-F.; Liu, F.; Liu, A.-Q.; Wang, Q.; Sun, H.-Y.; Wen, L.-X. Study of UV-Shielding Properties of Novel Porous Hollow Silica Nanoparticle Carriers for Avermectin. *Pest Manag. Sci.* **2007**, *63*, 241−246.

(31) Wibowo, D.; Zhao, C. X.; Peters, B. C.; Middelberg, A. P. J. Sustained Release of Fipronil Insecticide in Vitro and in Vivo from Biocompatible Silica Nanocapsules. *J. Agric. Food Chem.* **2014**, *62* (52), 12504−12511.

(32) Song, M. R.; Cui, S. M.; Gao, F.; Liu, Y. R.; Fan, C. L.; Lei, T. Q.; Liu, D. C. Dispersible Silica Nanoparticles as Carrier for Enhanced Bioactivity of Chlorfenapyr. *J. Pestic. Sci.* **2012**, *37* (3), 258−260.

(33) Ao, M.; Zhu, Y.; He, S.; Li, D.; Li, P.; Li, J.; Cao, Y. Preparation and Characterization of 1-Naphthylacetic Acid-Silica Conjugated Nanospheres for Enhancement of Controlled-Release Performance. *Nanotechnology* **2013**, *24* (3), 035601.

(34) Cao, L.; Zhou, Z.; Niu, S.; Cao, C.; Li, X.; Shan, Y.; Huang, Q. Positive-Charge Functionalized Mesoporous Silica Nanoparticles as Nanocarriers for Controlled 2,4-Dichlorophenoxy Acetic Acid Sodium Salt Release. *J. Agric. Food Chem.* **2018**, *66* (26), 6594−6603.

(35) Zobir bin Hussein, M.; Yahaya, A. H.; Zainal, Z.; Kian, L. H. Nanocomposite-Based Controlled Release Formulation of an Herbicide, 2,4-Dichlorophenoxyacetate Incapsulated in Zinc-Aluminium-Layered Double Hydroxide. *Sci. Technol. Adv. Mater.* **2005**, *6* (8), 956−962.

(36) Feizi, H.; Kamali, M.; Jafari, L.; Rezvani Moghaddam, P. Phytotoxicity and Stimulatory Impacts of Nanosized and Bulk

https://doi.org/10.1021/acsami.2c00615
ACS Appl. Mater. Interfaces 2022, 14, 16983−17007

Titanium Dioxide on Fennel (Foeniculum Vulgare Mill). *Chemosphere* **2013**, *91* (4), 506−511.
(37) Sarlak, N.; Taherifar, A.; Salehi, F. Synthesis of Nanopesticides by Encapsulating Pesticide Nanoparticles Using Functionalized Carbon Nanotubes and Application of New Nanocomposite for Plant Disease Treatment. *J. Agric. Food Chem.* **2014**, *62* (21), 4833−4838.
(38) Sharma, S.; Singh, S.; Ganguli, A. K.; Shanmugam, V. Anti-Drift Nano-Stickers Made of Graphene Oxide for Targeted Pesticide Delivery and Crop Pest Control. *Carbon N. Y.* **2017**, *115*, 781−790.
(39) Álvarez-Paino, M.; Muñoz-Bonilla, A.; Fernández-García, M. Antimicrobial Polymers in the Nano-World. *Nanomaterials* **2017**, *7* (2), 48.
(40) Li, H.; Eddaoudi, M.; O'Keeffe, M.; Yaghi, O. M. Design and Synthesis of an Exceptionally Stable and Highly Porous Metal-Organic Frameworks. *Nature* **1999**, *402* (18), 276−279.
(41) Zhang, Z.; Zhao, Y.; Gong, Q.; Li, Z.; Li, J. MOFs for CO2 Capture and Separation from Flue Gas Mixtures: The Effect of Multifunctional Sites on Their Adsorption Capacity and Selectivity. *Chem. Commun.* **2013**, *49* (7), 653−661.
(42) Madden, D.; Babu, R.; Camur, C.; Rampal, N.; Silvestre-Albero, J.; Curtin, T.; Fairen-Jimenez, D. Monolithic Metal-Organic Frameworks for Carbon Dioxide Separation. *Faraday Discuss.* **2021**, *231*, 51.
(43) García-Valdivia, A. A.; Pérez-Yáñez, S.; García, J. A.; Fernández, B.; Cepeda, J.; Rodríguez-Diéguez, A. Magnetic and Photoluminescent Sensors Based on Metal-Organic Frameworks Built up from 2-Aminoisonicotinate. *Sci. Rep.* **2020**, *10* (1), 1−17.
(44) Leo, P.; Briones, D.; Garciá, J. A.; Cepeda, J.; Orcajo, G.; Calleja, G.; Rodríguez-Diéguez, A.; Martínez, F. Strontium-Based MOFs Showing Dual Emission: Luminescence Thermometers and Toluene Sensors. *Inorg. Chem.* **2020**, *59* (24), 18432−18443.
(45) Salcedo-Abraira, P.; Santiago-Portillo, A.; Atienzar, P.; Bordet, P.; Salles, F.; Guillou, N.; Elkaim, E.; Garcia, H.; Navalon, S.; Horcajada, P. A Highly Conductive Nanostructured PEDOT Polymer Confined into the Mesoporous MIL-100(Fe). *Dalt. Trans.* **2019**, *48* (26), 9807−9817.
(46) Pascanu, V.; González Miera, G.; Inge, A. K.; Martín-Matute, B. Metal-Organic Frameworks as Catalysts for Organic Synthesis: A Critical Perspective. *J. Am. Chem. Soc.* **2019**, *141* (18), 7223−7234.
(47) Vilela, S.; Devic, T.; Varez, A.; Salles, F.; Horcajada, P. A New Proton-Conducting Bi-Carboxylate Framework. *Dalt. Trans.* **2019**, *48*, 11181−11185.
(48) Rojas, S.; Arenas-Vivo, A.; Horcajada, P. Metal-Organic Frameworks: A Novel Platform for Combined Advanced Therapies. *Coord. Chem. Rev.* **2019**, *388*, 202−226.
(49) Dias, E. M.; Petit, C. Towards the Use of Metal-Organic Frameworks for Water Reuse: A Review of the Recent Advances in the Field of Organic Pollutants Removal and Degradation and the next Steps in the Field. *J. Mater. Chem. A* **2015**, *3*, 22484−22506.
(50) Tang, J.; Ma, X.; Yang, J.; Feng, D. D.; Wang, X. Q. Recent Advances in Metal-Organic Frameworks for Pesticide Detection and Adsorption. *Dalt. Trans.* **2020**, *49* (41), 14361−14372.
(51) Mondol, M. M. H.; Jhung, S. H. Adsorptive Removal of Pesticides from Water with Metal-Organic Framework-Based Materials. *Chem. Eng. J.* **2021**, *421* (P1), 129688.
(52) Rojas, S.; Horcajada, P. Metal-Organic Frameworks for the Removal of Emerging Organic Contaminants in Water. *Chem. Rev.* **2020**, *120* (16), 8378−8415.
(53) Mon, M.; Bruno, R.; Ferrando-Soria, J.; Armentano, D.; Pardo, E. Metal-Organic Framework Technologies for Water Remediation: Towards a Sustainable Ecosystem. *J. Mater. Chem. A* **2018**, *6* (12), 4912−4947.
(54) Xu, Y.; Wang, H.; Li, X.; Zeng, X.; Du, Z.; Cao, J.; Jiang, W. Metal-Organic Framework for the Extraction and Detection of Pesticides from Food Commodities. *Compr. Rev. Food Sci. Food Saf.* **2021**, *20* (1), 1009−1035.
(55) Kumar, P.; Kim, K. H.; Deep, A. Recent Advancements in Sensing Techniques Based on Functional Materials for Organophosphate Pesticides. *Biosens. Bioelectron.* **2015**, *70*, 469−481.
(56) Anstoetz, M.; Rose, T. J.; Clark, M. W.; Yee, L. H.; Raymond, C. A.; Vancov, T. Novel Applications for Oxalate-Phosphate-Amine Metal-Organic-Frameworks (OPA-MOFs): Can an Iron-Based OPA-MOF Be Used as Slow-Release Fertilizer? *PLoS One* **2015**, *10*, 1−16.
(57) Jung, B. K.; Hasan, Z.; Jhung, S. H. Adsorptive Removal of 2,4-Dichlorophenoxyacetic Acid (2,4-D) from Water with a Metal-Organic Framework. *Chem. Eng. J.* **2013**, *234*, 99−105.
(58) Yang, Y.; Che, J.; Wang, B.; Wu, Y.; Chen, B.; Gao, L.; Dong, X.; Zhao, J. Visible-Light-Mediated Guest Trapping in a Photosensitizing Porous Coordination Network: Metal-Free C-C Bond-Forming Modification of Metal-Organic Frameworks for Aqueous-Phase Herbicide Adsorption. *Chem. Commun.* **2019**, *55* (37), 5383−5386.
(59) Liang, W.; Wang, B.; Cheng, J.; Xiao, D.; Xie, Z.; Zhao, J. 3D, Eco-Friendly Metal-Organic Frameworks@carbon Nanotube Aerogels Composite Materials for Removal of Pesticides in Water. *J. Hazard. Mater.* **2021**, *401*, 123718.
(60) Pankajakshan, A.; Sinha, M.; Ojha, A. A.; Mandal, S. Water-Stable Nanoscale Zirconium-Based Metal - Organic Frameworks for the E Ff Ective Removal of Glyphosate from Aqueous Media. *ACS Omega* **2018**, *3*, 7832−7839.
(61) Akpinar, I.; Drout, R. J.; Islamoglu, T.; Kato, S.; Lyu, J.; Farha, O. K. Exploiting π-π Interactions to Design an Efficient Sorbent for Atrazine Removal from Water. *ACS Appl. Mater. Interfaces* **2019**, *11*, 6097−6103.
(62) Liu, J.; Xiong, W. H.; Ye, L. Y.; Zhang, W. S.; Yang, H. Developing a Novel Nanoscale Porphyrinic Metal-Organic Framework: A Bifunctional Platform with Sensitive Fluorescent Detection and Elimination of Nitenpyram in Agricultural Environment. *J. Agric. Food Chem.* **2020**, *68* (20), 5572−5578.
(63) Oladipo, A. A.; Vaziri, R.; Abureesh, M. A. Highly Robust AgIO3/MIL-53 (Fe) Nanohybrid Composites for Degradation of Organophosphorus Pesticides in Single and Binary Systems: Application of Artificial Neural Networks Modelling. *J. Taiwan Inst. Chem. Eng.* **2018**, *83*, 133−142.
(64) Khodkar, A.; Khezri, S. M.; Pendashteh, A. R.; Khoramnejadian, S.; Mamani, L. A Designed Experimental Approach for Photocatalytic Degradation of Paraquat Using α-Fe2O3@MIL-101(Cr)@TiO2 Based on Metal-Organic Framework. *Int. J. Environ. Sci. Technol.* **2019**, *16*, 5741−5756.
(65) Gao, X.; Zhai, Q.; Hu, M.; Li, S.; Song, J.; Jiang, Y. Design and Preparation of Stable CPO/HRP@H-MOF(Zr) Composites for Efficient Bio-Catalytic Degradation of Organic Toxicants in Wastewater. *J. Chem. Technol. Biotechnol.* **2019**, *94* (4), 1249−1258.
(66) Yu, T.; Ma, H.; Zhang, H.; Xiong, M.; Liu, Y.; Li, F. Fabrication and Characterization of Purified Esterase-Embedded Zeolitic Imidazolate Frameworks for the Removal and Remediation of Herbicide Pollution from Soil. *J. Environ. Manage.* **2021**, *288* (April), 112450.
(67) Negro, C.; Martínez Pérez-Cejuela, H.; Simó-Alfonso, E. F.; Herrero-Martínez, J. M.; Bruno, R.; Armentano, D.; Ferrando-Soria, J.; Pardo, E. Highly Efficient Removal of Neonicotinoid Insecticides by Thioether-Based (Multivariate) Metal-Organic Frameworks. *ACS Appl. Mater. Interfaces* **2021**, *13* (24), 28424−28432.
(68) Ahmad, M.; Chen, S.; Ye, F.; Quan, X.; Afzal, S.; Yu, H.; Zhao, X. Efficient Photo-Fenton Activity in Mesoporous MIL-100(Fe) Decorated with ZnO Nanosphere for Pollutants Degradation. *Appl. Catal. B Environ.* **2019**, *245*, 428−438.
(69) Akpinar, I.; Yazaydin, A. O. Adsorption of Atrazine from Water in Metal-Organic Framework Materials. *J. Chem. Eng. Data* **2018**, *63* (7), 2368−2375.
(70) De Smedt, C.; Spanoghe, P.; Biswas, S.; Leus, K.; Van Der Voort, P. Comparison of Different Solid Adsorbents for the Removal of Mobile Pesticides from Aqueous Solutions. *Adsorption* **2015**, *21* (3), 243−254.
(71) Xiao, Y.; Chen, C.; Wu, Y.; Wang, J.; Yin, Y.; Chen, J.; Huang, X.; Qi, P.; Zheng, B. Water-Stable Al-TCPP MOF Nanosheets with Hierarchical Porous Structure for Removal of Chlorantraniliprole in Water. *Microporous Mesoporous Mater.* **2021**, *324* (May), 111272.

https://doi.org/10.1021/acsami.2c00615
ACS Appl. Mater. Interfaces 2022, 14, 16983−17007

(72) Abdelhameed, R. M.; Shaltout, A. A.; Mahmoud, M. H. H.; Emam, H. E. Efficient Elimination of Chlorpyrifos via Tailored Macroporous Membrane Based on Al-MOF. *Sustain. Mater. Technol.* **2021**, *29*, No. e00326.
(73) Fan, C.; Dong, H.; Liang, Y.; Yang, J.; Tang, G.; Zhang, W.; Cao, Y. Sustainable Synthesis of HKUST-1 and Its Composite by Biocompatible Ionic Liquid for Enhancing Visible-Light Photocatalytic Performance. *J. Clean. Prod.* **2019**, *208*, 353−362.
(74) Sarker, M.; Ahmed, I.; Jhung, S. H. Adsorptive Removal of Herbicides from Water over Nitrogen-Doped Carbon Obtained from Ionic Liquid@ZIF-8. *Chem. Eng. J.* **2017**, *323*, 203−211.
(75) Abazari, R.; Salehi, G.; Mahjoub, A. R. Ultrasound-Assisted Preparation of a Nanostructured Zinc(II) Amine Pillar Metal-Organic Framework as a Potential Sorbent for 2,4-Dichlorophenol Adsorption from Aqueous Solution. *Ultrason. Sonochem.* **2018**, *46*, 59−67.
(76) Wu, G.; Ma, J.; Li, S.; Wang, S.; Jiang, B.; Luo, S.; Li, J.; Wang, X.; Guan, Y.; Chen, L. Cationic Metal-Organic Frameworks as an Efficient Adsorbent for the Removal of 2,4-Dichlorophenoxyacetic Acid from Aqueous Solutions. *Environ. Res.* **2020**, *186*, 109542.
(77) Huang, X.; Feng, S.; Zhu, G.; Zheng, W.; Shao, C.; Zhou, N.; Meng, Q. Removal of Organic Herbicides from Aqueous Solution by Ionic Liquid Modified Chitosan/Metal-Organic Framework Composite. *Int. J. Biol. Macromol.* **2020**, *149*, 882−892.
(78) Mirsoleimani-Azizi, S. M.; Setoodeh, P.; Samimi, F.; Shadmehr, J.; Hamedi, N.; Rahimpour, M. R. Diazinon Removal from Aqueous Media by Mesoporous MIL-101(Cr) in a Continuous Fixed-Bed System. *J. Environ. Chem. Eng.* **2018**, *6* (4), 4653−4664.
(79) Diab, K. E.; Salama, E.; Hassan, H. S.; El-Moneim, A. A.; Elkady, M. F. Bio-Zirconium Metal-Organic Framework Regenerable Bio-Beads for the Effective Removal of Organophosphates from Polluted Water. *Polymers (Basel).* **2021**, *13*, 3869.
(80) Hlophe, P. V.; Dlamini, L. N. Photocatalytic Degradation of Diazinon with a 2d/3d Nanocomposite of Black Phosphorous/Metal Organic Framework. *Catalysts* **2021**, *11* (6), 679.
(81) Sheikhi, Z. N.; Khajeh, M.; Oveisi, A. R.; Bohlooli, M. Functionalization of an Iron-Porphyrinic Metal-Organic Framework with Bovine Serum Albumin for Effective Removal of Organophosphate Insecticides. *J. Mol. Liq.* **2021**, *343*, 116974.
(82) Jamali, A.; Shemirani, F.; Morsali, A. A Comparative Study of Adsorption and Removal of Organophosphorus Insecticides from Aqueous Solution by Zr-Based MOFs. *J. Ind. Eng. Chem.* **2019**, *80*, 83−92.
(83) Abdelhameed, R. M.; Abdel-Gawad, H.; Emam, H. E. Macroporous Cu-MOF@cellulose Acetate Membrane Serviceable in Selective Removal of Dimethoate Pesticide from Wastewater. *J. Environ. Chem. Eng.* **2021**, *9* (2), 105121.
(84) Abdelhameed, R. M.; Taha, M.; Abdel-Gawad, H.; Hegazi, B. Amino-Functionalized Al-MIL-53 for Dimethoate Pesticide Removal from Wastewater and Their Intermolecular Interactions. *J. Mol. Liq.* **2021**, *327*, 114852.
(85) Abdelhameed, R. M.; Abdel-Gawad, H.; Elshahat, M.; Emam, H. E. Cu-BTC@cotton Composite: Design and Removal of Ethion Insecticide from Water. *RSC Adv.* **2016**, *6* (48), 42324−42333.
(86) Abdelhameed, R. M.; Taha, M.; Abdel-Gawad, H.; Mahdy, F.; Hegazi, B. Zeolitic Imidazolate Frameworks: Experimental and Molecular Simulation Studies for Efficient Capture of Pesticides from Wastewater. *J. Environ. Chem. Eng.* **2019**, *7* (6), 103499.
(87) González, L.; Carmona, F. J.; Padial, N. M.; Navarro, J. A. R.; Barea, E.; Maldonado, C. R. Dual Removal and Selective Recovery of Phosphate and an Organophosphorus Pesticide from Water by a Zr-Based Metal-Organic Framework. *Mater. Today Chem.* **2021**, *22*, 100596.
(88) Ashouri, V.; Adib, K.; Rahimi Nasrabadi, M. A New Strategy for the Adsorption and Removal of Fenitrothion from Real Samples by Active-Extruded MOF (AE-MOF UiO-66) as an Adsorbent. *New J. Chem.* **2021**, *45* (11), 5029−5039.
(89) Li, T.; Lu, M.; Gao, Y.; Huang, X.; Liu, G.; Xu, D. Double Layer MOFs M-ZIF-8@ZIF-67: The Adsorption Capacity and Removal Mechanism of Fipronil and Its Metabolites from Environmental Water and Cucumber Samples. *J. Adv. Res.* **2020**, *24*, 159−166.
(90) Drout, R. J.; Kato, S.; Chen, H.; Son, F. A.; Otake, K. I.; Islamoglu, T.; Snurr, R. Q.; Farha, O. K. Isothermal Titration Calorimetry to Explore the Parameter Space of Organophosphorus Agrochemical Adsorption in MOFs. *J. Am. Chem. Soc.* **2020**, *142* (28), 12357−12366.
(91) Zhu, X.; Li, B.; Yang, J.; Li, Y.; Zhao, W.; Shi, J.; Gu, J. Effective Adsorption and Enhanced Removal of Organophosphorus Pesticides from Aqueous Solution by Zr-Based MOFs of UiO-67. *ACS Appl. Mater. Interfaces* **2015**, *7* (1), 223−231.
(92) Yang, Q.; Wang, J.; Zhang, W.; Liu, F.; Yue, X.; Liu, Y.; Yang, M.; Li, Z.; Wang, J. Interface Engineering of Metal Organic Framework on Graphene Oxide with Enhanced Adsorption Capacity for Organophosphorus Pesticide. *Chem. Eng. J.* **2017**, *313*, 19−26.
(93) Feng, D.; Xia, Y. Comparisons of Glyphosate Adsorption Properties of Different Functional Cr-Based Metal-Organic Frameworks. *J. Sep. Sci.* **2018**, *41* (3), 732−739.
(94) Yang, Q.; Wang, J.; Chen, X.; Yang, W.; Pei, H.; Hu, N.; Li, Z.; Suo, Y.; Li, T.; Wang, J. The Simultaneous Detection and Removal of Organophosphorus Pesticides by a Novel Zr-MOF Based Smart Adsorbent. *J. Mater. Chem. A* **2018**, *6* (5), 2184−2192.
(95) Chen, M. L.; Lu, T. H.; Li, S. S.; Wen, L.; Xu, Z.; Cheng, Y. H. Photocatalytic Degradation of Imidacloprid by Optimized Bi2WO6/NH2-MIL-88B(Fe) Composite under Visible Light. *Environ. Sci. Pollut. Res.* **2022**, *29* (13), 19583−19593.
(96) Seo, Y. S.; Khan, N. A.; Jhung, S. H. Adsorptive Removal of Methylchlorophenoxypropionic Acid from Water with a Metal-Organic Framework. *Chem. Eng. J.* **2015**, *270*, 22−27.
(97) Bansal, P.; Bharadwaj, L. M.; Deep, A.; K, P. Zn Based Metal Organic Framework as Adsorbent Material for Mecoprop. *Res. J. Recent Sci.* **2013**, *2* (7), 84−86.
(98) Bužek, D.; Demel, J.; Lang, K. Zirconium Metal-Organic Framework UiO-66: Stability in an Aqueous Environment and Its Relevance for Organophosphate Degradation. *Inorg. Chem.* **2018**, *57* (22), 14290−14297.
(99) Lange, L. E.; Ochanda, F. O.; Obendorf, S. K.; Hinestroza, J. P. CuBTC Metal-Organic Frameworks Enmeshed in Polyacrylonitrile Fibrous Membrane Remove Methyl Parathion from Solutions. *Fibers Polym.* **2014**, *15* (2), 200−207.
(100) Shadmehr, J.; Sedaghati, F.; Zeinali, S. Efficient Elimination of Propiconazole Fungicide from Aqueous Environments by Nanoporous MIL-101(Cr): Process Optimization and Assessment. *Int. J. Environ. Sci. Technol.* **2021**, *101*, 2937.
(101) Wei, Y.; Wang, B.; Cui, X.; Muhammad, Y.; Zhang, Y.; Huang, Z.; Li, X.; Zhao, Z.; Zhao, Z. Highly Advanced Degradation of Thiamethoxam by Synergistic Chemisorption-Catalysis Strategy Using MIL(Fe)/Fe-SPC Composites with Ultrasonic Irradiation. *ACS Appl. Mater. Interfaces* **2018**, *10* (41), 35260−35272.
(102) Liu, G.; Li, L.; Xu, D.; Huang, X.; Xu, X.; Zheng, S.; Zhang, Y.; Lin, H. Metal-Organic Framework Preparation Using Magnetic Graphene Oxide-*β*-Cyclodextrin for Neonicotinoid Pesticide Adsorption and Removal. *Carbohydr. Polym.* **2017**, *175*, 584−591.
(103) Liu, G.; Li, L.; Huang, X.; Zheng, S.; Xu, X.; Liu, Z.; Zhang, Y.; Wang, J.; Lin, H.; Xu, D. Adsorption and Removal of Organophosphorus Pesticides from Environmental Water and Soil Samples by Using Magnetic Multi-Walled Carbon Nanotubes @ Organic Framework ZIF-8. *J. Mater. Sci.* **2018**, *53* (15), 10772−10783.
(104) Anstoetz, M.; Sharma, N.; Clark, M.; Yee, L. H. Characterization of an Oxalate-Phosphate-Amine Metal-Organic Framework (OPA-MOF) Exhibiting Properties Suited for Innovative Applications in Agriculture. *J. Mater. Sci.* **2016**, *51* (20), 9239−9252.
(105) Yang, J.; Trickett, C. A.; Alahmadi, S. B.; Alshammari, A. S.; Yaghi, O. M. Calcium L-Lactate Frameworks as Naturally Degradable Carriers for Pesticides. *J. Am. Chem. Soc.* **2017**, *139* (24), 8118−8121.
(106) Tang, J.; Ding, G.; Niu, J.; Zhang, W.; Tang, G.; Liang, Y.; Fan, C.; Dong, H.; Yang, J.; Li, J.; Cao, Y. Preparation and Characterization of Tebuconazole Metal-Organic Framework-Based

https://doi.org/10.1021/acsami.2c00615
ACS Appl. Mater. Interfaces 2022, 14, 16983−17007

Microcapsules with Dual-Microbicidal Activity. *Chem. Eng. J.* **2019**, *359*, 225−232.
(107) Dong, J.; Chen, W.; Feng, J.; Liu, X.; Xu, Y.; Wang, C.; Yang, W.; Du, X. Facile, Smart, and Degradable Metal-Organic Framework Nanopesticides Gated with FeIII-Tannic Acid Networks in Response to Seven Biological and Environmental Stimuli. *ACS Appl. Mater. Interfaces* **2021**, *13* (16), 19507−19520.
(108) Tang, J.; Tang, G.; Niu, J.; Yang, J.; Zhou, Z.; Gao, Y.; Chen, X.; Tian, Y.; Li, Y.; Li, J.; Cao, Y. Preparation of a Porphyrin Metal-Organic Framework with Desirable Photodynamic Antimicrobial Activity for Sustainable Plant Disease Management. *J. Agric. Food Chem.* **2021**, *69* (8), 2382−2391.
(109) Shan, Y.; Cao, L.; Muhammad, B.; Xu, B.; Zhao, P.; Cao, C.; Huang, Q. Iron-Based Porous Metal-Organic Frameworks with Crop Nutritional Function as Carriers for Controlled Fungicide Release. *J. Colloid Interface Sci.* **2020**, *566*, 383−393.
(110) Chen, H.; Shan, Y.; Cao, L.; Zhao, P.; Cao, C.; Li, F.; Huang, Q. Enhanced Fungicidal Efficacy by Co-Delivery of Azoxystrobin and Diniconazole with Cauliflower-like Metal-Organic Frameworks NH2-Al-MIL-101. *Int. J. Mol. Sci.* **2021**, *22*, 10412.
(111) Meng, W.; Tian, Z.; Yao, P.; Fang, X.; Wu, T.; Cheng, J.; Zou, A. Preparation of a Novel Sustained-Release System for Pyrethroids by Using Metal-Organic Frameworks (MOFs) Nanoparticle. *Colloids Surfaces A Physicochem. Eng. Asp.* **2020**, *604* (May), 125266.
(112) Gao, Y.; Liang, Y.; Zhou, Z.; Yang, J.; Tian, Y.; Niu, J.; Tang, G.; Tang, J.; Chen, X.; Li, Y.; Cao, Y. Metal-Organic Framework Nanohybrid Carrier for Precise Pesticide Delivery and Pest Management. *Chem. Eng. J.* **2021**, *422* (2), 130143.
(113) Shan, Y.; Xu, C.; Zhang, H.; Chen, H.; Bilal, M.; Niu, S.; Cao, L.; Huang, Q. Polydopamine-Modified Metal-Organic Frameworks, NH2-Fe-MIL-101, as PH-Sensitive Nanocarriers for Controlled Pesticide Release. *Nanomaterials* **2020**, *10* (10), 2000.
(114) Feng, P.; Chen, J.; Fan, C.; Huang, G.; Yu, Y.; Wu, J.; Lin, B. An Eco-Friendly MIL-101@CMCS Double-Coated Dinotefuran for Long-Acting Active Release and Sustainable Pest Control. *J. Clean. Prod.* **2020**, *265*, 121851.
(115) Ji, Y.; Ma, S.; Lv, S.; Wang, Y.; Lü, S.; Liu, M. Nanomaterials for Targeted Delivery of Agrochemicals by an All-in-One Combination Strategy and Deep Learning. *ACS Appl. Mater. Interfaces* **2021**, *13*, 43374−43386.
(116) Yang, J.; Dai, D.; Cai, Z.; Liu, Y. Q.; Qin, J. C.; Wang, Y.; Yang, Y. W. MOF-Based Multi-Stimuli-Responsive Supramolecular Nanoplatform Equipped with Macrocycle Nanovalves for Plant Growth Regulation. *Acta Biomater.* **2021**, *134*, 664−673.
(117) Meng, W.; Gao, Y.; Tian, Z.; Xu, W.; Cheng, J.; Li, S.; Zou, A. Fe3O4Magnetic Cores Coated with Metal-Organic Framework Shells as Collectable Composite Nanoparticle Vehicles for Sustained Release of the Pesticide Imidacloprid. *ACS Appl. Nano Mater.* **2021**, *4* (6), 5864−5870.
(118) Wu, C.; Dan, Y.; Tian, D.; Zheng, Y.; Wei, S.; Xiang, D. Facile Fabrication of MOF(Fe)@alginate Aerogel and Its Application for a High-Performance Slow-Release N-Fertilizer. *Int. J. Biol. Macromol.* **2020**, *145*, 1073−1079.
(119) Mejías, F. J. R.; Trasobares, S.; Varela, R. M.; Molinillo, J. M. G.; Calvino, J. J.; Macías, F. A. One-Step Encapsulation of Ortho-Disulfides in Functionalized Zinc MOF. Enabling Metal-organic Frameworks in Agriculture. *ACS Appl. Mater. Interfaces* **2021**, *13* (7), 7997−8005.
(120) Liang, W.; Xie, Z.; Cheng, J.; Xiao, D.; Xiong, Q.; Wang, Q.; Zhao, J.; Gui, W. A Light-Triggered PH-Responsive Metal-Organic Framework for Smart Delivery of Fungicide to Control Sclerotinia Diseases of Oilseed Rape. *ACS Nano* **2021**, *15* (4), 6987−6997.
(121) Huang, G.; Deng, Y.; Zhang, Y.; Feng, P.; Xu, C.; Fu, L.; Lin, B. Study on Long-Term Pest Control and Stability of Double-Layer Pesticide Carrier in Indoor and Outdoor Environment. *Chem. Eng. J.* **2021**, *403*, 126342.
(122) Wen, L. L.; Wang, F.; Leng, X. K.; Wang, C. G.; Wang, L. Y.; Gong, J. M.; Li, D. F. Efficient Detection of Organophosphate Pesticide Based on a Metal-Organic Framework Derived from Biphenyltetracarboxylic Acid. *Cryst. Growth Des.* **2010**, *10* (7), 2835−2838.
(123) Barreto, A. S.; Da Silva, R. L.; Dos Santos Silva, S. C. G.; Rodrigues, M. O.; De Simone, C. A.; De Sá, G. F.; Júnior, S. A.; Navickiene, S.; De Mesquita, M. E. Potential of a Metal-Organic Framework as a New Material for Solid-Phase Extraction of Pesticides from Lettuce (Lactuca Sativa), with Analysis by Gas Chromatography-Mass Spectrometry. *J. Sep. Sci.* **2010**, *33* (23−24), 3811−3816.
(124) Tao, C. L.; Chen, B.; Liu, X. G.; Zhou, L. J.; Zhu, X. L.; Cao, J.; Gu, Z. G.; Zhao, Z.; Shen, L.; Tang, B. Z. A Highly Luminescent Entangled Metal-Organic Framework Based on Pyridine-Substituted Tetraphenylethene for Efficient Pesticide Detection. *Chem. Commun.* **2017**, *53* (72), 9975−9978.
(125) He, K.; Li, Z.; Wang, L.; Fu, Y.; Quan, H.; Li, Y.; Wang, X.; Gunasekaran, S.; Xu, X. A Water-Stable Luminescent Metal-Organic Framework for Rapid and Visible Sensing of Organophosphorus Pesticides. *ACS Appl. Mater. Interfaces* **2019**, *11* (29), 26250−26260.
(126) Zhang, S.; Jiao, Z.; Yao, W. A Simple Solvothermal Process for Fabrication of a Metal-Organic Framework with an Iron Oxide Enclosure for the Determination of Organophosphorus Pesticides in Biological Samples. *J. Chromatogr. A* **2014**, *1371*, 74−81.
(127) Niu, M.; Li, Z.; He, W.; Zhou, W.; Lu, R.; Li, J.; Gao, H.; Zhang, S.; Pan, C. Attapulgite Modified Magnetic Metal-Organic Frameworks for Magnetic Solid Phase Extraction and Determinations of Benzoylurea Insecticides in Tea Infusions. *Food Chem.* **2020**, *317*, 126425.
(128) Senosy, I. A.; Guo, H. M.; Ouyang, M. N.; Lu, Z. H.; Yang, Z. H.; Li, J. H. Magnetic Solid-Phase Extraction Based on Nano-Zeolite Imidazolate Framework-8-Functionalized Magnetic Graphene Oxide for the Quantification of Residual Fungicides in Water, Honey and Fruit Juices. *Food Chem.* **2020**, *325*, 126944.
(129) Tu, X.; Gao, F.; Ma, X.; Zou, J.; Yu, Y.; Li, M.; Qu, F.; Huang, X.; Lu, L. Mxene/Carbon Nanohorn/β-Cyclodextrin-Metal-Organic Frameworks as High-Performance Electrochemical Sensing Platform for Sensitive Detection of Carbendazim Pesticide. *J. Hazard. Mater.* **2020**, *396* (April), 122776.
(130) Zhang, S.; Du, Z.; Li, G. Metal-Organic Framework-199/Graphite Oxide Hybrid Composites Coated Solid-Phase Microextraction Fibers Coupled with Gas Chromatography for Determination of Organochlorine Pesticides from Complicated Samples. *Talanta* **2013**, *115* (2), 32−39.
(131) Soury, S.; Firoozichahak, A.; Nematollahi, D.; Alizadeh, S.; Kakaei, H.; Abbasi, A. Needle-Trap Device Packed with the MIL-100(Fe) Metal-Organic Framework for the Extraction of the Airborne Organochlorine Pesticides. *Microchem. J.* **2021**, *171*, 106866.
(132) Jiang, Y.; Ma, P.; Li, X.; Piao, H.; Li, D.; Sun, Y.; Wang, X.; Song, D. Application of Metal-Organic Framework MIL-101(Cr) to Microextraction in Packed Syringe for Determination of Triazine Herbicides in Corn Samples by Liquid Chromatography-Tandem Mass Spectrometry. *J. Chromatogr. A* **2018**, *1574*, 36−41.
(133) Li, N.; Wu, L.; Nian, L.; Song, Y.; Lei, L.; Yang, X.; Wang, K.; Wang, Z.; Zhang, L.; Zhang, H.; Yu, A.; Zhang, Z. Dynamic Microwave Assisted Extraction Coupled with Dispersive Micro-Solid-Phase Extraction of Herbicides in Soybeans. *Talanta* **2015**, *142*, 43−50.
(134) Li, N.; Wang, Z.; Zhang, L.; Nian, L.; Lei, L.; Yang, X.; Zhang, H.; Yu, A. Liquid-Phase Extraction Coupled with Metal-Organic Frameworks-Based Dispersive Solid Phase Extraction of Herbicides in Peanuts. *Talanta* **2014**, *128*, 345−353.
(135) Nasrollahpour, A.; Moradi, S. E. A Simple Vortex-Assisted Magnetic Dispersive Solid Phase Microextraction System for Preconcentration and Separation of Triazine Herbicides from Environmental Water and Vegetable Samples Using Fe3O4@MIL-100(Fe) Sorbent. *J. AOAC Int.* **2018**, *101*, 1639−1646.
(136) Yang, J. H.; Zhou, X. M.; Zhang, Y. P.; Chen, J.; Ma, H. W. A Novel Method for the Determination of Trace Sulfonylurea Herbicides by Introducing a Hybrid Stationary Phase to Common Capillary. *Adsorpt. Sci. Technol.* **2017**, *35* (3−4), 372−385.

https://doi.org/10.1021/acsami.2c00615
ACS Appl. Mater. Interfaces 2022, 14, 16983−17007

(137) Yang, J. H.; Cui, C. X.; Qu, L. B.; Chen, J.; Zhou, X. M.; Zhang, Y. P. Preparation of a Monolithic Magnetic Stir Bar for the Determination of Sulfonylurea Herbicides Coupled with HPLC. *Microchem. J.* **2018**, *141* (1), 369−376.
(138) Jin, R.; Ji, F.; Lin, H.; Luo, C.; Hu, Y.; Deng, C.; Cao, X.; Tong, C.; Song, G. The Synthesis of Zr-Metal-Organic Framework Functionalized Magnetic Graphene Nanocomposites as an Adsorbent for Fast Determination of Multi-Pesticide Residues in Tobacco Samples. *J. Chromatogr. A* **2018**, *1577*, 1−7.
(139) Liang, L.; Wang, X.; Sun, Y.; Ma, P.; Li, X.; Piao, H.; Jiang, Y.; Song, D. Magnetic Solid-Phase Extraction of Triazine Herbicides from Rice Using Metal-Organic Framework MIL-101(Cr) Functionalized Magnetic Particles. *Talanta* **2018**, *179*, 512−519.
(140) Zhou, L.; Su, P.; Deng, Y.; Yang, Y. Self-Assembled Magnetic Nanoparticle Supported Zeolitic Imidazolate Framework-8: An Efficient Adsorbent for the Enrichment of Triazine Herbicides from Fruit, Vegetables, and Water. *J. Sep. Sci.* **2017**, *40* (4), 909−918.
(141) Xu, N.; Zhang, Q.; Hou, B.; Cheng, Q.; Zhang, G. A Novel Magnesium Metal-Organic Framework as a Multiresponsive Luminescent Sensor for Fe(III) Ions, Pesticides, and Antibiotics with High Selectivity and Sensitivity. *Inorg. Chem.* **2018**, *57* (21), 13330−13340.
(142) Santos Barreto, A.; de Cássia da Silva Andrade, P.; Meira Farias, J.; Menezes Filho, A.; Fernandes de Sá, G.; Alves Júnior, S. Characterization and Application of a Lanthanide-Based Metal-Organic Framework in the Development and Validation of a Matrix Solid-Phase Dispersion Procedure for Pesticide Extraction on Peppers (Capsicum Annuum L.) with Gas Chromatography-Mass Spectrometr. *J. Sep. Sci.* **2018**, *41* (7), 1593−1599.
(143) Wang, X.; Ma, X.; Wang, H.; Huang, P.; Du, X.; Lu, X. A Zinc(II) Benzenetricarboxylate Metal Organic Framework with Unusual Adsorption Properties, and Its Application to the Preconcentration of Pesticides. *Microchim. Acta* **2017**, *184* (10), 3681−3687.
(144) Singha, D. K.; Majee, P.; Mondal, S. K.; Mahata, P. Detection of Pesticide Using the Large Stokes Shift of Luminescence of a Mixed Lanthanide Co-Doped Metal-Organic Framework. *Polyhedron* **2019**, *158*, 277−282.
(145) Singha, D. K.; Majee, P.; Mondal, S. K.; Mahata, P. Highly Selective Aqueous Phase Detection of Azinphos-Methyl Pesticide in Ppb Level Using a Cage-Connected 3D MOF. *ChemistrySelect* **2017**, *2* (20), 5760−5768.
(146) Singha, D. K.; Majee, P.; Mandal, S.; Mondal, S. K.; Mahata, P. Detection of Pesticides in Aqueous Medium and in Fruit Extracts Using a Three-Dimensional Metal-Organic Framework: Experimental and Computational Study. *Inorg. Chem.* **2018**, *57* (19), 12155−12165.
(147) Ma, J.; Li, S.; Wu, G.; Wang, S.; Guo, X.; Wang, L.; Wang, X.; Li, J.; Chen, L. Preparation of Mixed-Matrix Membranes from Metal Organic Framework (MIL-53) and Poly (Vinylidene Fluoride) for Use in Determination of Sulfonylurea Herbicides in Aqueous Environments by High Performance Liquid Chromatography. *J. Colloid Interface Sci.* **2019**, *553*, 834−844.
(148) Deng, Y.; Zhang, R.; Li, D.; Sun, P.; Su, P.; Yang, Y. Preparation of Iron-Based MIL-101 Functionalized Polydopamine@ Fe3O4Magnetic Composites for Extracting Sulfonylurea Herbicides from Environmental Water and Vegetable Samples. *J. Sep. Sci.* **2018**, *41* (9), 2046−2055.
(149) Xu, X.; Wang, X.; Liu, M.; Tan, T.; Wan, Y. ZIF-8@SiO2 Core-Shell Microsphere Extraction Coupled with Liquid Chromatography and Triple Quadrupole Tandem Mass Spectrometry for the Quantitative Analysis of Four Plant Growth Regulators in Navel Oranges. *J. Sep. Sci.* **2018**, *41* (18), 3561−3568.
(150) Mao, X.; Xiao, W.; Wan, Y.; Li, Z.; Luo, D.; Yang, H. Dispersive Solid-Phase Extraction Using Microporous Metal-Organic Framework UiO-66: Improving the Matrix Compounds Removal for Assaying Pesticide Residues in Organic and Conventional Vegetables. *Food Chem.* **2021**, *345*, 128807.
(151) Lu, N.; He, X.; Wang, T.; Liu, S.; Hou, X. Magnetic Solid-Phase Extraction Using MIL-101(Cr)-Based Composite Combined with Dispersive Liquid-Liquid Microextraction Based on Solidification of a Floating Organic Droplet for the Determination of Pyrethroids in Environmental Water and Tea Samples. *Microchem. J.* **2018**, *137*, 449−455.
(152) dos Anjos de Jesus, R.; Santos, L. F. S.; Navickiene, S.; de Mesquita, M. E. Evaluation of Metal-Organic Framework as Low-Cost Adsorbent Material in the Determination of Pesticide Residues in Soursop Exotic Fruit (Annona Muricata) by Liquid Chromatography. *Food Anal. Methods* **2015**, *8* (2), 446−451.
(153) de Jesus, J. R.; Wanderley, K. A.; Alves Júnior, S.; Navickiene, S. Evaluation of a Novel Metal-Organic Framework as an Adsorbent for the Extraction of Multiclass Pesticides from Coconut Palm (Cocos Nucifera L.): An Analytical Approach Using Matrix Solid-Phase Dispersion and Liquid Chromatography. *J. Sep. Sci.* **2017**, *40* (16), 3327−3334.
(154) Zhang, C.; Zhang, L.; Yu, R. Extraction and Separation of Acetanilide Herbicides in Beans Based on Metal-Organic Framework MIL-101(Zn) as Sorbent. *Food Addit. Contam. - Part A* **2019**, *36* (11), 1677−1687.
(155) Wang, X. M.; Kou, H.; Wang, J.; Teng, R.; Du, X.; Lu, X. An Octahedral Magnetic Metal Organic Frameworks for Efficient Extraction and Enrichment of Six Pesticides with Benzene Ring Prior to High Performance Liquid Chromatography Analysis. *J. Porous Mater.* **2020**, *27* (4), 1171−1177.
(156) Han, Y.; He, X.; Yang, W.; Luo, X.; Yu, Y.; Tang, W.; Yue, T.; Li, Z. Ratiometric Fluorescent Sensing Carbendazim in Fruits and Vegetables via Its Innate Fluorescence Coupling with UiO-67. *Food Chem.* **2021**, *345*, 128839.
(157) Soltani-Shahrivar, M.; Karimian, N.; Fakhri, H.; Hajian, A.; Afkhami, A.; Bagheri, H. Design and Application of a Non-Enzymatic Sensor Based on Metal-Organic Frameworks for the Simultaneous Determination of Carbofuran and Carbaryl in Fruits and Vegetables. *Electroanalysis* **2019**, *31* (12), 2455−2465.
(158) Fan, M. Y.; Yu, H. H.; Fu, P.; Su, Z. M.; Li, X.; Hu, X. L.; Gao, F. W.; Pan, Q. Q. Luminescent Cd(II) Metal-Organic Frameworks with Anthracene Nitrogen-Containing Organic Ligands as Novel Multifunctional Chemosensors for the Detection of Picric Acid, Pesticides, and Ferric Ions. *Dye. Pigment.* **2021**, *185*, 108834.
(159) Amiripour, F.; Ghasemi, S.; Azizi, S. N. Design of Turn-on Luminescent Sensor Based on Nanostructured Molecularly Imprinted Polymer-Coated Zirconium Metal-Organic Framework for Selective Detection of Chloramphenicol Residues in Milk and Honey. *Food Chem.* **2021**, *347*, 129034.
(160) Di, L.; Xia, Z.; Li, J.; Geng, Z.; Li, C.; Xing, Y.; Yang, Z. Selective Sensing and Visualization of Pesticides by ABW-Type Metal-Organic Framework Based Luminescent Sensors. *RSC Adv.* **2019**, *9* (66), 38469−38476.
(161) Nagabooshanam, S.; Sharma, S.; Roy, S.; Mathur, A.; Krishnamurthy, S.; Bharadwaj, L. M. Development of Field Deployable Sensor for Detection of Pesticide from Food Chain. *IEEE Sens. J.* **2021**, *21* (4), 4129−4134.
(162) Liu, Q.; Wang, H.; Han, P.; Feng, X. Fluorescent Aptasensing of Chlorpyrifos Based on the Assembly of Cationic Conjugated Polymer-Aggregated Gold Nanoparticles and Luminescent Metal-Organic Frameworks. *Analyst* **2019**, *144* (20), 6025−6032.
(163) Wei, W.; Wang, J.; Tian, C. B.; Du, S. W.; Wu, K. C. A Highly Hydrolytically Stable Lanthanide Organic Framework as a Sensitive Luminescent Probe for DBP and Chlorpyrifos Detection. *Analyst* **2018**, *143* (22), 5481−5486.
(164) Karami, K.; Mardaniboldaji, A.; Rezayat, M. R.; Bayat, P.; Jafari, M. T. Novel UiO-66-NH2/Gly/GO Nanocomposite Adsorbent for Ultra-Trace Analyzing of Chlorpyrifos Pesticide by Ion Mobility Spectrometry. *ChemistrySelect* **2021**, *6* (14), 3370−3377.
(165) Shen, B.; Ma, C.; Ji, Y.; Dai, J.; Li, B.; Zhang, X.; Huang, H. Detection of Carboxylesterase 1 and Chlorpyrifos with ZIF-8 Metal-Organic Frameworks Using a Red Emission BODIPY-Based Probe. *ACS Appl. Mater. Interfaces* **2021**, *13* (7), 8718−8726.
(166) Bagheri, H.; Amanzadeh, H.; Yamini, Y.; Masoomi, M. Y.; Morsali, A.; Salar-Amoli, J.; Hassan, J. A Nanocomposite Prepared from a Zinc-Based Metal-Organic Framework and Polyethersulfone as

https://doi.org/10.1021/acsami.2c00615
ACS Appl. Mater. Interfaces 2022, 14, 16983−17007

a Novel Coating for the Headspace Solid-Phase Microextraction of Organophosphorous Pesticides. *Microchim. Acta* **2018**, *185* (62), 1−8.
(167) Amini, S.; Amiri, M.; Ebrahimzadeh, H.; Seidi, S.; Hejabri kandeh, S. Synthesis of Magnetic Cu/CuFe2O4@MIL-88A(Fe) Nanocomposite and Application to Dispersive Solid-Phase Extraction of Chlorpyrifos and Phosalone in Water and Food Samples. *J. Food Compos. Anal.* **2021**, *104*, 104128.
(168) Jia, Y.; Wang, Y.; Yan, M.; Wang, Q.; Xu, H.; Wang, X.; Zhou, H.; Hao, Y.; Wang, M. Fabrication of Iron Oxide@MOF-808 as a Sorbent for Magnetic Solid Phase Extraction of Benzoylurea Insecticides in Tea Beverages and Juice Samples. *J. Chromatogr. A* **2020**, *1615*, 460766.
(169) Jin, D.; Xu, Q.; Yu, L.; Hu, X. Photoelectrochemical Detection of the Herbicide Clethodim by Using the Modified Metal-Organic Framework Amino-MIL-125(Ti)/TiO2. *Microchim. Acta* **2015**, *182* (11−12), 1885−1892.
(170) Liang, T.; Wang, S.; Chen, L.; Niu, N. Metal Organic Framework-Molecularly Imprinted Polymer as Adsorbent in Matrix Solid Phase Dispersion for Pyrethroids Residue Extraction from Wheat. *Food Anal. Methods* **2019**, *12* (1), 217−228.
(171) Si, T.; Liu, L.; Liang, X.; Duo, H.; Wang, L.; Wang, S. Solid-Phase Extraction of Phenoxyacetic Acid Herbicides in Complex Samples with a Zirconium(IV)-Based Metal-Organic Framework. *J. Sep. Sci.* **2019**, *42* (12), 2148−2154.
(172) Su, Y.; Wang, S.; Zhang, N.; Cui, P.; Gao, Y.; Bao, T. Zr-MOF Modified Cotton Fiber for Pipette Tip Solid-Phase Extraction of Four Phenoxy Herbicides in Complex Samples. *Ecotoxicol. Environ. Saf.* **2020**, *201* (May), 110764.
(173) Duo, H.; Wang, Y.; Wang, L.; Lu, X.; Liang, X. Zirconium-(IV)-Based Metal-Organic Frameworks (UiO-67) as Solid-Phase Extraction Adsorbents for Extraction of Phenoxyacetic Acid Herbicides from Vegetables. *J. Sep. Sci.* **2018**, *41* (22), 4149−4158.
(174) Xia, L.; Liu, L.; Xu, X.; Zhu, F.; Wang, X.; Zhang, K.; Yang, X.; You, J. Determination of Chlorophenoxy Acid Herbicides by Using a Zirconium-Based Metal-Organic Framework as Special Sorbent for Dispersive Micro-Solid-Phase Extraction and High- Performance Liquid Chromatography. *New J. Chem.* **2017**, *41* (6), 2241−2248.
(175) Huang, X.; Liu, G.; Xu, D.; Xu, X.; Li, L.; Zheng, S.; Lin, H.; Gao, H. Novel Zeolitic Imidazolate Frameworks Based on Magnetic Multiwalled Carbon Nanotubes for Magnetic Solid-Phase Extraction of Organochlorine Pesticides from Agricultural Irrigation Water Samples. *Appl. Sci.* **2018**, *8* (6), 959.
(176) Ashouri, V.; Adib, K.; Nasrabadi, M. R.; Ghalkhani, M. Preparation of the Extruded UiO-66-Based Metal-Organic Framework for the Diazinon Removal from the Real Samples. *J. Mol. Struct.* **2021**, *1240*, 130607.
(177) Darvishnejad, F.; Raoof, J. B.; Ghani, M. MIL-101 (Cr) @ Graphene Oxide-Reinforced Hollow Fiber Solid-Phase Microextraction Coupled with High-Performance Liquid Chromatography to Determine Diazinon and Chlorpyrifos in Tomato, Cucumber and Agricultural Water. *Anal. Chim. Acta* **2020**, *1140*, 99−110.
(178) Amiri, A.; Tayebee, R.; Abdar, A.; Narenji Sani, F. Synthesis of a Zinc-Based Metal-Organic Framework with Histamine as an Organic Linker for the Dispersive Solid-Phase Extraction of Organophosphorus Pesticides in Water and Fruit Juice Samples. *J. Chromatogr. A* **2019**, *1597*, 39−45.
(179) Liu, G.; Tian, M.; Lu, M.; Shi, W.; Li, L.; Gao, Y.; Li, T.; Xu, D. Preparation of Magnetic MOFs for Use as a Solid-Phase Extraction Absorbent for Rapid Adsorption of Triazole Pesticide Residues in Fruits Juices and Vegetables. *J. Chromatogr. B Anal. Technol. Biomed. Life Sci.* **2021**, *1166*, 122500.
(180) Guo, X. Y.; Dong, Z. P.; Zhao, F.; Liu, Z. L.; Wang, Y. Q. Zinc(II)-Organic Framework as a Multi-Responsive Photoluminescence Sensor for Efficient and Recyclable Detection of Pesticide 2,6-Dichloro-4-Nitroaniline, Fe(III) and Cr(VI). *New J. Chem.* **2019**, *43* (5), 2353−2361.
(181) Fan, L.; Wang, F.; Zhao, D.; Sun, X.; Chen, H.; Wang, H.; Zhang, X. Two Cadmium(II) Coordination Polymers as Multi-Functional Luminescent Sensors for the Detection of Cr(VI) Anions, Dichloronitroaniline Pesticide, and Nitrofuran Antibiotic in Aqueous Media. *Spectrochim. Acta - Part A Mol. Biomol. Spectrosc.* **2020**, *239*, 118467.
(182) Xu, N.; Zhang, Q.; Zhang, G. A Carbazole-Functionalized Metal-Organic Framework for Efficient Detection of Antibiotics, Pesticides and Nitroaromatic Compounds. *Dalt. Trans.* **2019**, *48* (8), 2683−2691.
(183) Feng, D. D.; Zhao, Y. Di; Wang, X. Q.; Fang, D. D.; Tang, J.; Fan, L. M.; Yang, J. Two Novel Metal-Organic Frameworks Based on Pyridyl-Imidazole-Carboxyl Multifunctional Ligand: Selective CO2 Capture and Multiresponsive Luminescence Sensor. *Dalt. Trans.* **2019**, *48* (29), 10892−10900.
(184) Wang, X. Q.; Ma, X.; Feng, D.; Tang, J.; Wu, D.; Yang, J.; Jiao, J. Four Novel Lanthanide(III) Metal-Organic Frameworks: Tunable Light Emission and Multiresponsive Luminescence Sensors for Vitamin B6and Pesticides. *Cryst. Growth Des.* **2021**, *21* (5), 2889−2897.
(185) Wang, G. D.; Li, Y. Z.; Shi, W. J.; Zhang, B.; Hou, L.; Wang, Y. Y. A Robust Cluster-Based Eu-MOF as Multi-Functional Fluorescence Sensor for Detection of Antibiotics and Pesticides in Water. *Sensors Actuators, B Chem.* **2021**, *331*, 129377.
(186) Liu, G.; Huang, X.; Lu, M.; Li, L.; Li, T.; Xu, D. Facile Synthesis of Magnetic Zinc Metal-Organic Framework for Extraction of Nitrogen-Containing Heterocyclic Fungicides from Lettuce Vegetable Samples. *J. Sep. Sci.* **2019**, *42* (7), 1451−1458.
(187) Yao, W.; Fan, Z.; Zhang, S. Preparation of Metal-Organic Framework UiO-66-Incorporated Polymer Monolith for the Extraction of Trace Levels of Fungicides in Environmental Water and Soil Samples. *J. Sep. Sci.* **2019**, *42* (16), 2679−2686.
(188) Zhang, S.; Yang, Q.; Wang, W.; Wang, C.; Wang, Z. Covalent Bonding of Metal-Organic Framework-5/Graphene Oxide Hybrid Composite to Stainless Steel Fiber for Solid-Phase Microextraction of Triazole Fungicides from Fruit and Vegetable Samples. *J. Agric. Food Chem.* **2016**, *64* (13), 2792−2801.
(189) Zhang, S.; Hua, Z.; Zhao, H.; Yao, W.; Wu, Y.; Fu, D.; Sun, J. Defective Zr-Based Metal-Organic Frameworks as Sorbent for the Determination of Fungicides in Environmental Water Samples by Rapid Dispersive Micro-Solid-Phase Extraction Coupled to Liquid Chromatography/Mass Spectrometry. *J. Sep. Sci.* **2021**, *44* (10), 2113−2120.
(190) Jiao, Z. H.; Hou, S. L.; Kang, X. M.; Yang, X. P.; Zhao, B. Recyclable Luminescence Sensor for Dinotefuran in Water by Stable Cadmium-Organic Framework. *Anal. Chem.* **2021**, *93* (17), 6599−6603.
(191) Kumar, P.; Paul, A. K.; Deep, A. A Luminescent Nanocrystal Metal Organic Framework for Chemosensing of Nitro Group Containing Organophosphate Pesticides. *Anal. Methods* **2014**, *6* (12), 4095−4101.
(192) Kumar, P.; Paul, A. K.; Deep, A. Sensitive Chemosensing of Nitro Group Containing Organophosphate Pesticides with MOF-5. *Microporous Mesoporous Mater.* **2014**, *195*, 60−66.
(193) Guselnikova, O.; Postnikov, P.; Elashnikov, R.; Miliutina, E.; Svorcik, V.; Lyutakov, O. Metal-Organic Framework (MOF-5) Coated SERS Active Gold Gratings: A Platform for the Selective Detection of Organic Contaminants in Soil. *Anal. Chim. Acta* **2019**, *1068*, 70−79.
(194) Yu, C. X.; Hu, F. L.; Song, J. G.; Zhang, J. L.; Liu, S. S.; Wang, B. X.; Meng, H.; Liu, L. L.; Ma, L. F. Ultrathin Two-Dimensional Metal-Organic Framework Nanosheets Decorated with Tetra-Pyridyl Calix[4]Arene: Design, Synthesis and Application in Pesticide Detection. *Sensors Actuators, B Chem.* **2020**, *310*, 127819.
(195) Li, Y.; Wu, S.; Zhang, Y.; Ma, Z.; Zhu, M.; Gao, E. A Lanthanide Metal-Organic Framework as Ratio Fluorescence Probe to Detect Pesticides in Water. *Inorg. Chim. Acta* **2021**, *528*, 120632.
(196) Smith, K. T.; Ramsperger, C. A.; Hunter, K. E.; Zuehlsdorff, T. J.; Stylianou, K. C. Colorimetric Detection of Acidic Pesticides in Water. *Chem. Commun.* **2022**, *58* (7), 953−956.
(197) Xu, Y.; Li, X.; Zhang, W.; Jiang, H.; Pu, Y.; Cao, J.; Jiang, W. Zirconium(IV)-Based Metal-Organic Framework for Determination

https://doi.org/10.1021/acsami.2c00615
ACS Appl. Mater. Interfaces 2022, 14, 16983−17007

of Imidacloprid and Thiamethoxam Pesticides from Fruits by UPLC-MS/MS. *Food Chem.* **2021**, *344*, 128650.
(198) Huang, Y. F.; Liu, Q. H.; Li, K.; Li, Y.; Chang, N. Magnetic Iron(III)-Based Framework Composites for the Magnetic Solid-Phase Extraction of Fungicides from Environmental Water Samples. *J. Sep. Sci.* **2018**, *41* (5), 1129−1137.
(199) Al'Abri, A. M.; Abdul Halim, S. N.; Abu Bakar, N. K.; Saharin, S. M.; Sherino, B.; Rashidi Nodeh, H.; Mohamad, S. Highly Sensitive and Selective Determination of Malathion in Vegetable Extracts by an Electrochemical Sensor Based on Cu-Metal Organic Framework. *J. Environ. Sci. Heal. - Part B Pestic. Food Contam. Agric. Wastes* **2019**, *54* (12), 930−941.
(200) Habila, M.; Alhenaki, B.; El-Marghany, A.; Sheikh, M.; Ghfar, A.; ALOthman, Z.; Soylak, M. Metal Organic Frameworks Enhanced Dispersive Solid Phase Microextraction of Malathion before Detection by UHPLC-MS/MS. *J. Sep. Sci.* **2020**, *43* (15), 3103−3109.
(201) Ma, L.; He, Y.; Wang, Y.; Wang, Y.; Li, R.; Huang, Z.; Jiang, Y.; Gao, J. Nanocomposites of Pt Nanoparticles Anchored on UiO66-NH2 as Carriers to Construct Acetylcholinesterase Biosensors for Organophosphorus Pesticide Detection. *Electrochim. Acta* **2019**, *318*, 525−533.
(202) Mohammadnejad, M.; Gudarzi, Z.; Geranmayeh, S.; Mahdavi, V. HKUST-1 Metal-Organic Framework for Dispersive Solid Phase Extraction of 2-Methyl-4-Chlorophenoxyacetic Acid (MCPA) Prior to Its Determination by Ion Mobility Spectrometry. *Microchim. Acta* **2018**, *185* (10), 1−8.
(203) Li, D.; Zhang, X.; Kong, F.; Qiao, X.; Xu, Z. Molecularly Imprinted Solid-Phase Extraction Coupled with High-Performance Liquid Chromatography for the Determination of Trace Trichlorfon and Monocrotophos Residues in Fruits. *Food Anal. Methods* **2017**, *10* (5), 1284−1292.
(204) Davoodi, M.; Davar, F.; Rezayat, M. R.; Jafari, M. T.; Bazarganipour, M.; Shalan, A. E. Synthesis and Characterization of a New ZIF-67@MgAl2O4nanocomposite and Its Adsorption Behaviour. *RSC Adv.* **2021**, *11* (22), 13245−13255.
(205) Gao, G.; Liu, W.; Liu, G.; Zhu, M.; Zhang, Y.; Wu, S.; Gao, E. A Water-Stable Tb(III) Metal-Organic Framework with Multiple Fluorescent Centers for Efficient Self-Calibration Sensing Pesticides. *ChemistrySelect* **2021**, *6* (39), 10481−10488.
(206) Cheng, C.; Shen, C.; Lai, O. M.; Tan, C. P.; Cheong, L. Z. Biomimetic Self-Assembly of Lipase-Zeolitic Imidazolate Frameworks with Enhanced Biosensing of Protox Inhibiting Herbicides. *Anal. Methods* **2021**, *13* (42), 4974−4984.
(207) Bai, W.; Qin, G.; Wang, J.; Li, L.; Ni, Y. 2-Aminoterephthalic Acid Co-Coordinated Co-MOF Fluorescent Probe for Highly Selective Detection of the Organophosphorus Pesticides with p-Nitrophenyl Group in Water Systems. *Dye. Pigment.* **2021**, *193* (March), 109473.
(208) Xu, X.; Guo, Y.; Wang, X.; Li, W.; Qi, P.; Wang, Z.; Wang, X.; Gunasekaran, S.; Wang, Q. Sensitive Detection of Pesticides by a Highly Luminescent Metal-Organic Framework. *Sensors Actuators, B Chem.* **2018**, *260*, 339−345.
(209) Zhu, A.; Xuan, T.; Zhai, Y.; Wu, Y.; Guo, X.; Ying, Y.; Wen, Y.; Yang, H. Preparation of Magnetic Metal Organic Framework: A Magnetically Induced Improvement Effect for Detection of Parathion-Methyl. *Sensors Actuators, B Chem.* **2021**, *339* (March), 129909.
(210) Gao, N.; Tan, R.; Cai, Z.; Zhao, H.; Chang, G.; He, Y. A Novel Electrochemical Sensor via Zr-Based Metal Organic Framework-Graphene for Pesticide Detection. *J. Mater. Sci.* **2021**, *56* (34), 19060−19074.
(211) Li, J.; Weng, Y.; Shen, C.; Luo, J.; Yu, D.; Cao, Z. Sensitive Fluorescence and Visual Detection of Organophosphorus Pesticides with a Ru(Bpy)32+-ZIF-90-MnO2sensing Platform. *Anal. Methods* **2021**, *13* (26), 2981−2988.
(212) Chen, H.; Fan, P.; Tu, X.; Min, H.; Yu, X.; Li, X.; Zeng, J. L.; Zhang, S.; Cheng, P. A Bifunctional Luminescent Metal-Organic Framework for the Sensing of Paraquat and Fe3+ Ions in Water. *Chem. - An Asian J.* **2019**, *14* (20), 3611−3619.
(213) Deep, A.; Bhardwaj, S. K.; Paul, A. K.; Kim, K. H.; Kumar, P. Surface Assembly of Nano-Metal Organic Framework on Amine Functionalized Indium Tin Oxide Substrate for Impedimetric Sensing of Parathion. *Biosens. Bioelectron.* **2015**, *65*, 226−231.
(214) Bera, M. K.; Behera, L.; Mohapatra, S. A Fluorescence Turn-down-up Detection of Cu2+ and Pesticide Quinalphos Using Carbon Quantum Dot Integrated UiO-66-NH2. *Colloids Surfaces A Physicochem. Eng. Asp.* **2021**, *624* (April), 126792.
(215) Yang, L.; Liu, Y. L.; Liu, C. G.; Ye, F.; Fu, Y. Two Luminescent Dye@MOFs Systems as Dual-Emitting Platforms for Efficient Pesticides Detection. *J. Hazard. Mater.* **2020**, *381*, 120966.
(216) Peng, X. X.; Bao, G. M.; Zhong, Y. F.; Zhang, L.; Zeng, K. B.; He, J. X.; Xiao, W.; Xia, Y. F.; Fan, Q.; Yuan, H. Q. Highly Sensitive and Rapid Detection of Thiabendazole Residues in Oranges Based on a Luminescent Tb3+-Functionalized MOF. *Food Chem.* **2021**, *343*, 128504.
(217) Xuan, T.; Gao, Y.; Cai, Y.; Guo, X.; Wen, Y.; Yang, H. Fabrication and Characterization of the Stable Ag-Au-Metal-Organic-Frameworks: An Application for Sensitive Detection of Thiabendazole. *Sensors Actuators, B Chem.* **2019**, *293* (May), 289−295.
(218) Mueller, U.; Schubert, M.; Teich, F.; Puetter, H.; Schierle-Arndt, K.; Pastré, J. Metal-Organic Frameworks—Prospective Industrial Applications. *J. Mater. Chem.* **2006**, *16*, 626−636.

https://doi.org/10.1021/acsami.2c00615
ACS Appl. Mater. Interfaces 2022, 14, 16983−17007